CORE
Metadata, citation and similar papers at core.ac.uk
Provided by ethesis@nitr

Speed Sensorless Field Oriented Control of Induction Motor through Speed and Flux estimation

A Thesis submitted in partial fulfillment of the requirements for the degree of Master of Technology in Power Electronics and drives

by

SADANANDA MAJHI

Roll no.-213EE4327

Under the Guidance of:

Prof. K. B. MOHANTY

Department of Electrical Engineering

National Institute of Technology Rourkela

ODISHA -769008, INDIA

Speed Sensorless Field Oriented Control of Induction Motor through Speed and Flux estimation

A Thesis submitted in partial fulfillment of the requirements for the degree of Master of Technology in Power Electronics and drives

by

SADANANDA MAJHI

Roll no.-213EE4327

Under the Guidance of:

Prof. K. B. MOHANTY

Department of Electrical Engineering

National Institute of Technology Rourkela

ODISHA -769008, INDIA

Dedicated to my beloved parents and my all family Members.

DEPARTMENT OF ELECTRICAL ENGINEERING

NATIONAL INSTITUTE OF TECHNOLOGY, ROURKELA

ODISHA, INDIA-769008

CERTIFICATE

This is to certify that the thesis entitled "**Speed Sensorless Field Oriented Control of Induction Motor through Speed and Flux Estimation**", submitted by Mr. Sadananda Majhi bearing Roll No. 213EE4327, in partial fulfilment of the requirements for the award of Master of Technology in Electrical Engineering with specialization in "Power Electronics and Drives" during session 2013-2015 at National Institute of Technology, Rourkela is an authentic of work carried out by him under my supervision and guidance.

To the best of my knowledge, the matter embodied in the thesis has not been submitted to any other university/institute for the award of any Degree or Diploma.

Date:

Place: Rourkela

Prof. K. B. MOHANTY

Dept. of Electrical Engineering

National Institute of Technology

Rourkela- 769008

ACKNOWLEDGMENTS

I would like to express my sincere gratitude to my supervisor **Prof. K. B. Mohanty** for his guidance, encouragement, and support throughout the course of this work. It was an invaluable learning experience for me to be one of their students. From them I have gained not only extensive knowledge, but also a careful research attitude.

I express my gratitude to **Prof. A. K. Panda,** Head of the Department, Electrical Engineering for his invaluable suggestions and constant encouragement all through the thesis work.

My thanks are extended to my colleagues in power control and drives, who built an academic and friendly research environment that made my study at NIT, Rourkela most fruitful and enjoyable.

Finally I would also like to acknowledge the entire teaching and non-teaching staff of Electrical department for establishing a working environment and for constructive discussions.

SADANANDA MAJHI
Roll no.:- 213EE4327
M. Tech (PED)

ABSTRACT

Separately excited dc motors were used in industry for high performance applications and servo applications. This was due to simple control of dc motor contrasted with an ac motor. Now days dc motors have been replaced by the induction motors for high performance applications because induction motors are cheaper, robust and have low moment of inertia and light weight. The entry of vector control strategies the control of an induction motor is changed into that of a separately excited dc motor. In vector control torque and flux can be controlled independently. Accepting that the rotor flux position is known the stator current phases are resolved along and in quadrature to it. The quadrature component of stator current is the torque current, $i_{\beta s}$ and the in phase component of stator current is field current, $i_{\alpha s}$. The transformation of current requires unit vectors which are derived from the rotor flux signals. When the measured field angle is used to determine unit vector in the vector control scheme is known as direct vector control and that using evaluated field angle is called indirect vector control scheme.

In conventional vector control a rotational transducer is used to sense the speed. It increases complexity of the drives and decreases reliability of the system. In some cases it is undesirable such as high speed drives. But all these sensorless indirect vector control have a disadvantage that motor parameters variation with temperature causes an estimation speed error in steady state and transient state. This increases the losses of the motor and reduces efficiency of the drive. However, speed sensorless vector control based on rotor flux observer method has finite parameters variation effect and speed accuracy is improved by observer.

Efforts are being made to decrease the sensitivity of the drives system to motor parameters variation. The aim of this project work is to build up a vector controlled induction motor drive working without a speed sensor. The methodology is to detect the motor speed by using rotor flux observer. It estimates the stator currents and rotor flux by measuring terminal currents and voltages, and the speed is then estimated by utilizing the rotor flux and the current errors between the actual stator current and the estimated stator current.

CONTENTS

LIST OF SYMBOLS

The list of principal symbols used in the text given below

d - q	Synchronously rotating reference frame direct and quadrature axes
α - β	Stationary reference frame direct and quadrature axes
P	Number of poles
L_m	Magnetizing inductance
L_r	Rotor inductance
L_s	Stator inductance.
Ψ_r	Rotor flux linkage
Ψ_s	Stator flux linkage
Ψ_{dr}	d - axis rotor flux linkage
$\Psi_{\alpha r}$	α - axis rotor flux linkage
$\Psi_{\alpha s}$	α – axis stator flux linkage
Ψ_{qr}	q - axis rotor flux linkage
$\Psi_{\beta r}$	β - axis rotor flux linkage
$\Psi_{\beta s}$	β – axis stator flux linkage
i_{ds}	d – axis stator stator current
i_{qs}	q – axis stator stator current
$i_{\alpha s}$	α – axis stator current
$i_{\alpha r}$	α – axis rotor current
$i_{\beta s}$	β – axis stator current
$i_{\beta r}$	β – axis rotor current
$v_{\alpha s}$	α – axis stator voltage
$v_{\beta s}$	β – axis stator voltage
R_s	Stator resistance
R_r	Rotor resistance
ω_r	Rotor electrical speed
ω_m	Rotor mechanical speed
T_e	Developed torque (Nm)

LIST OF FIGURE

Chapter- 1

INTRODUCTION

1.1 Vector control of induction motor

Induction motor was invented by Nikola Tesla in 1888. He succeeded, after numerous years, at building up an alternating current machine that did not require brushes for its operation. This development marked an upset in electrical engineering and gave a decisive impulse to broad utilization of three phase generation and distribution system. Moreover the choice of present fundamental frequency (60Hz in the USA and 50 Hz in Europe) was built up in the late 19th century on the grounds that Tesla thought that it was suitable for his induction motors, and at the same time, 60 Hz was found to deliver no flickering when utilized for lighting application. At the present time more than 60% of all the electrical energy produced on the planet is utilized by cage induction motors. Nevertheless induction machines have been generally utilized for fixed speed application over a century. Whereas, dc machines have been utilized for variable speed operation using the Ward- Leonard configuration. This method requires 3 machine (2 DC machine and 1 induction machine) and therefore it is unreasonable, bigger and requires maintenance.

Power electronics provides variable speed drive for both the DC and AC machine. The previous normally utilized thyristor controlled rectifier to offer superior torque, speed and flux control. PWM technique is used to produce polyphase supply for the induction motor (IM) drives. The greater part of these IM drives are taking into account keeping a constant voltage/frequency (v/f) ratio so as to keep up steady flux. Although, the dynamic performance of torque and flux of v/f drives is very poor, the control of v/f is moderately simple. As a result, a great quantity of industrial applications use dc machine because it provides good torque, speed and position control. The advantage of induction machine are clear as far as in expense and robustness, on the other hand, it was not until the execution and advancement of vector control that induction machines were able to content with DC machine in high performance applications. The machine flux and torque can be controlled independently in vector (field orientation) control, in a comparative way to separately excited DC machine.

The principle of vector control for high performance control of machines was

developed in Germany. Two possible approaches for achieving vector control were identified. Blaschke used Hall transducer mounted in the air gap to sense the machine flux, and therefore obtain the flux magnitude and flux angle for field orientation in vector control. Field orientation achieved by direct measurement of the flux is termed Direct Flux Orientation (DFO). Whereas Hasse achieved flux orientation by imposing a slip frequency derived from the rotor dynamic equations so as to ensure field orientation. This alternative, consisting of forcing field orientation in the machine, is known as Indirect Field Orientation (IFO). IFO has been generally preferred to DFO implementations which use Hall probes; the reason being that DFO requires a specially modified machine and moreover the fragility of the Hall sensors detracts the inherent robustness of an induction machine.

The operation of IFO requires correct alignment of the d-q reference frame with the rotor flux vector. This needs an accurate knowledge of the machine rotor time constant (T_r). Temperature of the motor changes with operation which causes variation of rotor time constant. On-line identification of the secondary time constant for calculation of the correct slip frequency in Indirect Rotor Flux Orientation (IRFO) is essential. An IRFO drive with on-line tuning of T_r can provide better torque and speed dynamics than a typical DC drive.

1.2 Vector control without speed transducers

The use of vector controlled induction motor drives provides several advantages over DC machines in terms of size, robustness, lack of brushes, and maintenance and reduced cost. However the typical IRFO induction motor drive requires the use of an accurate shaft encoder for correct operation. The use of this encoder implies additional electronics, extra space, extra wiring and careful mounting which is undesirable for high performance applications. In addition at low powers (2 to 5 kW) the cost of the sensor is about the same as the motor. Even at 50 kW, it can still be between 20 to 30% of the machine cost. Therefore there has been great interest in the research community in developing a high performance induction motor drive that does not require a speed or position transducer for its operation.

Some kind of speed estimation is required for high performance motor drives, in order to perform speed control. Speed estimation from terminal quantities can be obtained either by exploiting magnetic saliencies in the machine or by using a machine model.

Speed estimation using magnetic saliencies, such as rotor slotting, rotor asymmetries or variations on the leakage reactance, is independent of machine parameters and can be considered a true speed measurement. However, these techniques cannot be used directly as speed feedback signal for high performance speed control, because they present relative large measurement delays or because they can only be used within a reduced range of frequencies.

Alternatively, speed information can be obtained by using a machine model fed by stator quantities. These include the use of simple open loop speed calculators, Model Reference Adaptive Systems (MRAS) and Extended Kalman Filters. All these methods are effected by the parameters variation, therefore parameter errors can degrade speed holding characteristics. However these systems provide fast speed estimation, suitable for direct use for speed feedback.

It must be remembered that a high performance inner torque control loop is also required. The inner torque loop can be obtained by utilizing Indirect Field Orientation using the rotor speed estimate from an MRAS [9] instead of the measured speed. However the use of a speed estimate for both speed control and for IFO makes the torque control loop sensitive to parameter errors in the MRAS speed estimator. A second option is to use a DFO inner loop whereby flux is measured using Hall probes, end windings or tapped stator windings. Clearly this demands the use of a modified machine and is unacceptable to drive manufacturers. Other strategies are only applicable to a particular machine configuration, like the use of the 3rd harmonic of the phase voltage to obtain the flux angle in star connected machines.

A third option is to derive the machine flux from a motor model, e.g. flux observers, the use of Extended Kalman Filters [11], and Extended Luenberger Observers. This broadens the definition of Direct Field Orientation to cover not only the methods of flux orientation that use a direct measurement of the flux, but also those that use a flux estimate for field orientation.

1.3 Literature review

Several sensorless vector control schemes for three phase induction motor such as slip calculation, model referencing adaptive system (MRAS), speed adaptive flux observer and Extended Kaman's filter (EKF) have been developed. However all these sensorless vector

control have a drawback that motor parameters vary with motor operation. The parameter variation causes an estimation error of the motor speed. Hence, rotor resistance estimation is essential for speed sensorless vector control of induction motor [1, 8, 16].

A model referencing adaptive system (MRAS) [9] estimates motor speed from measured terminal voltages and currents. The estimated speed is utilized as criticism as a part a vector control system, consequently accomplishing speed control without the utilization of shaft-mounted transducers. This method is not so much complex but rather more stable.

Speed sensorless vector control of induction motor using rotor flux observer [4, 5, 6, 10, 12, 18, 19] where the motor speed can be estimated by using rotor flux observer. An observer is basically an estimator that uses a plant model and a feedback loop with measured plant variables. It estimates the rotor flux and stator currents by using terminal voltages and currents and the speed is estimated from rotor flux. However, Speed adaptive flux observer for induction motor speed sensorless vector control is always unstable in the regenerating mode at low speeds [10]. Many strategies about stabilizing the speed adaptive flux observer are proposed. The relationship between the instability and the feedback gain matrix is revealed and a corresponding method is also proposed. There is a different feedback gain matrix method was also designed to reduce the instability problem.

A model of induction motor in view of voltage decoupling control principle for speed sensorless vector-controlled induction motor drive system [7] has been developed. The model comprises of two subsystems, the torque current and rotor flux subsystems, and is advantageously to tackle the issues of voltage coupling. As indicated by this model, a speed estimation technique is introduced for speed sensorless vector controlled induction motor drive system. Being utilized controlled voltage mode in light of current resource model of induction motor, the cross coupling of stator voltage equations in synchronously rotating reference frame cannot be cancelled. Therefore, the rotor flux and torque component of the stator current impact one another to impact the performance of system. To cancel the inner coupling action of induction motor so as to obtain decoupling item, a decoupling signal of input voltage commands of induction motor is added in between excitation and torque signal input port.

1.4 Motivation

Induction motor is one of the most widely used motors in the industry applications. It

is used in transportation and industries, and also in laboratories, and household applications. The major reasons behind the popularity of the Induction Motors are:

i. Induction Motors are cheap compared to DC Motors. In this age of competition, this is a prime requirement for any machine. Due to its economy of transportation and installation, the Induction Motor is usually the first choice for an operation.
ii. Induction Motors have high efficiency of energy conversion. Also they are very reliable
iii. Squirrel-Cage Induction Motors are very rugged in construction. The robustness enables them to be used in all kinds of environments and for long durations of time.
iv. Induction Motors have very high starting torque. Because of high starting torque, induction motors are useful in applications where the load is applied before starting the motor.
v. Due to their simplicity of construction, Induction Motors have very low maintenance cost.

Another major advantage of the Induction Motor over other motors is the speed of the motor can be controlled easily. Different applications require different optimum speeds for the motor to run at. Therefore, Speed control is essential in Induction Motors because of the following factors:

i. It assure smooth operation.
ii. It provides torque control and acceleration control.
iii. During installation, slow running of the motors is required.
iv. Different applications require the motor to run at different speeds.

All these factors present a strong case for the implementation of speed control or variable speed drives in Induction Motors.

1.5 Objective

The main aim of this research work is to implement and evaluate a high performance sensorless vector control drive. A rotor flux observer is employed to obtain flux and the speed is estimated to achieve field orientation and speed control. A classical vector control of induction motor achieves the decoupling between rotor flux and torque only at steady state, when the value of the rotor flux is constant. The constant power mode of operation of the drive above the base speed, requires flux weakening such that the input voltage remains at rated value. For maximum efficiency of the drive rotor flux has to be adjusted continuously depending on the rotor speed command. Under these conditions the

rotor flux and torque no longer decouple. Such changes in rotor flux causes undesirable disturbances in the rotor speed. A linearized control scheme is proposed for induction motor drive system to decouple the rotor flux and torque, even under the condition of flux transient.

Speed sensorless vector control of ac motor drives has drawn an attention of researchers, because of the demerits of the speed sensor like additional cost, reduce reliability and measurement noise. Although many sensorless control schemes and speed estimation schemes have been proposed during few past years, advancement of straightforward and low sensitive speed estimation scheme, for low power machine is deficient in literature.

All these sensorless vector control schemes have a disadvantage that the motor parameters variation causes estimation error under steady state and transient state. Therefore, it is also essential to estimate the motor parameters and speed simultaneously, but is very difficult to estimate the motor parameters and speed simultaneously. Efforts are being made to decrease the sensitivity of the drives system to motor parameters variations.

Speed measurement using the rotor flux observer is employed to enhance speed regulation. Therefore an important part of this research is directed towards the implementation of a Simulink model in order to obtain reliable and accurate speed information.

Operation below base speed with nominal value of motor parameters is assumed through the project and the analysis and implementation of the proposed sensorless vector controlled drive with parameters estimation is considered as a topic for further study.

1.6 Organization of thesis

The thesis is shorted out into six chapters including the introduction in the chapter 1. Each of these are summarized below.

Chapter 2: Deals with the state space modelling of induction motor in stationary reference frame and designing of rotor flux observer. Stator currents and rotor flux are considered as state variables.

Chapter 3: Deals with estimation schemes for speed and resistance**.** Also, the working principle of speed sensorless field oriented control scheme and hysteresis band current

controller for three phase induction motor are presented.

Chapter 4: Describes the method to convert variables from three phase to two phase quantities and variables transformation into stationary reference frame and also rotating reference frame.

Chapter 5: Summarizes all the simulation results obtained of speed sensorless vector control with load and without load in different speed and makes conclusion based on those results.

Chapter 6: Deals with the general conclusion of the project work.

Chapter- 2

MODELLING OF INDUCTION MOTOR AND DESIGN OF ROTOR FLUX OBSERVER

2.1 Introduction

The control of ac motor, particularly induction motor, in spite of their simple construction is more complicated compared to that of a dc motor, the reason being the state space model of induction motor is highly nonlinear. Therefore, the proper mathematical model of induction motor is required for the design and development of such drive systems.

In this chapter modeling of induction motor and design of rotor flux observer have been presented. The measurement of rotor flux is difficult and more complicated. It is also uneconomical to install flux sensing coils or Hall effect transducers and so observers are often used to estimate the flux. Study and design of rotor flux observer has been presented.

2.2 Dynamic model of induction motor

The model of three phase induction motor which is valid for both steady state as well as transient state is necessary to study and simulate overall drive system. The dynamic model of induction motor in the stationary reference frame can be described in [2.1- 2.23]. The model of induction motor is developed on stationary reference frame utilizing the following assumptions:

1. Saturation is neglected.
2. Stator windings are distributed.
3. Core losses and skin effect are neglected.
4. Mutual inductances are same.
5. The harmonic in currents and voltages are ignored.

The equations governing the voltage at stator terminals considering the stationary reference frame are shown below.

$$v_{\alpha s} = R_s i_{\alpha s} + \dot{\Psi}_{\alpha s} \tag{2.1}$$

$$v_{\beta s} = R_s i_{\beta s} + \dot{\Psi}_{\beta s} \tag{2.2}$$

The equations governing the voltage at rotor terminals in stationary frame are given as follows.

$$v_{\alpha r} = 0 = R_r i_{\alpha r} + \dot{\Psi}_{\alpha r} + \omega_r \Psi_{\beta r} \tag{2.3}$$

$$v_{\beta r} = 0 = R_r i_{\beta r} + \dot{\Psi}_{\beta r} - \omega_r \Psi_{dr} \tag{2.4}$$

Where Ψ is the flux linkage, V represents voltage, R is reserved for resistance, i denote the current and ω_r is the rotor speed. The subscript r denotes the rotor quantity, s referred to the stator quantity, and the subscripts α and β denotes direct axis and quadrature axis components respectively in the stationary reference frame.

The expressions for stator and rotor flux linkages are given below.

$$\Psi_{\alpha r} = L_m i_{\alpha s} + L_r i_{\alpha r} \tag{2.5}$$

$$\Psi_{\beta r} = L_m i_{\beta s} + L_r i_{\beta r} \tag{2.6}$$

$$\Psi_{\alpha s} = L_m i_{\alpha r} + L_s i_{\alpha s} \tag{2.7}$$

$$\Psi_{\beta s} = L_m i_{\beta r} + L_s i_{\beta s} \tag{2.8}$$

Where $L_m$is the magnetizing inductance, L_r is the rotor inductance referred to the stator and L_s is the stator inductance.

Torque generated by an induction motor is given by

$$T_e = \frac{3p}{4}\frac{L_m}{L_r}(\Psi_{dr} i_{qs} - \Psi_{qr} i_{ds}) \tag{2.9}$$

Where, Ψ_{dr} and Ψ_{qr} are the rotor flux linkages, subscript ‘d-q’ denoting direct axis and quadrature axis in synchronously rotating reference frame, i_{qs} and i_{ds} are the stator currents in synchronous frame, and p is the number of poles.

Using the field-oriented control principle, the current component i_{ds} is aligned with rotor flux vector $\overline{\Psi}_r$, and the current component i_{qs} is oriented in a direction perpendicular to it. This orientation is governed by the following equation.

$$\Psi_{qr} = 0 \quad , \quad \Psi_{dr} = |\overline{\Psi}_r| \tag{2.10}$$

So the expression of torque developed by the motor can be written as

$$T_e = \frac{3p}{4}\frac{L_m}{L_r}\Psi_{dr} i_{qs} = K_T i_{qs} \tag{2.11}$$

Where, $K_T$is the torque constant, which is given in equation (2.12).

$$K_T = \frac{3p}{4}\frac{L_m}{L_r}\Psi_{dr} \tag{2.12}$$

Where, Ψ_{dr} denotes the command rotor flux.

Eliminating i_{dr} and i_{qr} from Equation (3) and (4), respectively, with the help of Equation (5) and (6), we get

$$\dot{\Psi}_{\alpha r} = -\frac{R_r}{L_r}\Psi_{\alpha r} - \omega_r \Psi_{\beta r} + \frac{L_m R_r}{L_r} i_{\alpha s} \tag{2.13}$$

$$\dot{\Psi}_{\beta r} = -\frac{R_r}{L_r}\Psi_{\beta r} + \omega_r \Psi_{\alpha r} + \frac{L_m R_r}{L_r} i_{\beta s} \tag{2.14}$$

Eliminating i_{dr} and i_{qr} from Equation (7) and (8) using Equation (5) and (6), the following equations are deduced.

$$\Psi_{\alpha s} = \frac{L_m}{L_r}\Psi_{\alpha r} + L_s \sigma i_{\alpha s} \tag{2.15}$$

$$\Psi_{\beta s} = \frac{L_m}{L_r}\Psi_{\beta r} + L_s \sigma i_{\beta s} \tag{2.16}$$

Where $\sigma = 1 - \frac{L_m^2}{L_r L_s}$ is the motor leakage coefficient.

Now, substituting Equation (13) and (14) in Equation (1) and (2) and finding Ψ_{dr} and Ψ_{qr} , we obtain

$$\dot{\Psi}_{\alpha r} = \frac{L_r}{L_m} v_{\alpha s} - \frac{L_r}{L_m} R_s i_{\alpha s} - \frac{L_r}{L_m}\sigma L_s i_{\alpha s} \tag{2.17}$$

$$\dot{\Psi}_{\beta r} = \frac{L_r}{L_m} v_{\beta s} - \frac{L_r}{L_m} R_s i_{\beta s} - \frac{L_r}{L_m}\sigma L_s i_{\beta s} \tag{2.18}$$

Substituting Equation (13) and (14) in Equation (17) and (18), respectively, and simplifying, we get

$$\dot{i}_{\alpha s} = -\frac{L_m^2 R_r + L_r^2 R_s}{\sigma L_s L_r^2} i_{\alpha s} + \frac{L_m R_r}{\sigma L_s L_r^2}\Psi_{\alpha r} + \frac{L_m \omega_r}{\sigma L_s L_r}\Psi_{\beta r} + \frac{1}{\sigma L_s} v_{\alpha s} \tag{2.19}$$

$$\dot{i}_{\beta s} = -\frac{L_m^2 R_r + L_r^2 R_s}{\sigma L_s L_r^2} i_{\beta s} + \frac{L_m R_r}{\sigma L_s L_r^2}\Psi_{\beta r} - \frac{L_m \omega_r}{\sigma L_s L_r}\Psi_{\alpha r} + \frac{1}{\sigma L_s} v_{\beta s} \tag{2.20}$$

Now choosing the stator current and rotor flux as the state variables, the state equation of the induction motor in stationary frame is given as follows:

$$\begin{bmatrix} \dot{i}_{\alpha s} \\ \dot{i}_{\beta s} \\ \dot{\Psi}_{\alpha r} \\ \dot{\Psi}_{\beta r} \end{bmatrix} = \begin{bmatrix} -\rho & 0 & \frac{R_r}{cL_r} & \frac{\omega_r}{c} \\ 0 & -\rho & -\frac{\omega_r}{c} & \frac{R_r}{cL_r} \\ \frac{L_m R_r}{L_r} & 0 & -\frac{R_r}{L_r} & -\omega_r \\ 0 & \frac{L_m R_r}{L_r} & \omega_r & -\frac{R_r}{L_r} \end{bmatrix} \begin{bmatrix} i_{\alpha s} \\ i_{\beta s} \\ \Psi_{\alpha r} \\ \Psi_{\beta r} \end{bmatrix} + \begin{bmatrix} \frac{1}{\sigma L_s} & 0 \\ 0 & \frac{1}{\sigma L_s} \\ 0 & 0 \\ 0 & 0 \end{bmatrix} \begin{bmatrix} v_{\alpha s} \\ v_{\beta s} \end{bmatrix}$$

$$\begin{bmatrix} \dot{i}_{\alpha s} \\ \dot{i}_{\beta s} \\ \dot{\Psi}_{\alpha r} \\ \dot{\Psi}_{\beta r} \end{bmatrix} = \begin{bmatrix} -a_1 & 0 & a_2 & a_3\omega_r \\ 0 & -a_1 & -a_3\omega_r & a_2 \\ a_5 & 0 & -a_4 & -\omega_r \\ 0 & a_5 & \omega_r & -a_4 \end{bmatrix} \begin{bmatrix} i_{\alpha s} \\ i_{\beta s} \\ \Psi_{\alpha r} \\ \Psi_{\beta r} \end{bmatrix} + \begin{bmatrix} \frac{1}{\sigma L_s} & 0 \\ 0 & \frac{1}{\sigma L_s} \\ 0 & 0 \\ 0 & 0 \end{bmatrix} \begin{bmatrix} v_{\alpha s} \\ v_{\beta s} \end{bmatrix} \quad (2.21)$$

$$\dot{x} = Ax + Bv_s \quad (2.22)$$

Where,

$x = \begin{bmatrix} i_{\alpha s} & i_{\beta s} & \Psi_{\alpha r} & \Psi_{\beta r} \end{bmatrix}^T$,

$v_s = \begin{bmatrix} v_{\alpha s} & v_{\beta s} \end{bmatrix}^T$,

$$A = \begin{bmatrix} -\rho & 0 & \frac{R_r}{cL_r} & \frac{w_r}{c} \\ 0 & -\rho & -\frac{w_r}{c} & \frac{R_r}{cL_r} \\ \frac{L_m R_r}{L_r} & 0 & -\frac{R_r}{L_r} & -w_r \\ 0 & \frac{L_m R_r}{L_r} & w_r & -\frac{R_r}{L_r} \end{bmatrix},$$

$$B = \begin{bmatrix} \frac{1}{\sigma L_s} & 0 & 0 & 0 \\ 0 & \frac{1}{\sigma L_s} & 0 & 0 \end{bmatrix}^T,$$

$\rho = \frac{L_m^2 R_r + L_r^2 R_s}{\sigma L_s L_r^2}$,

$c = \frac{\sigma L_s L_r}{L_m}$,

$a_1 = \frac{L_m^2 R_r + L_r^2 R_s}{\sigma L_s L_r^2}$,

$a_2 = \frac{L_m R_r}{\sigma L_s L_r^2}$,

$a_3 = \frac{L_m}{\sigma L_s L_r}$,

$a_4 = \frac{R_r}{L_r}$ and

$a_5 = \frac{L_m R_r}{L_r}$.

The observer output is governed by Equation (2.23) where stator current is considered as the output.

$$y = Cx \tag{2.23}$$

Where, $C = \begin{bmatrix} 1 & 0 & 0 & 0 \\ 0 & 1 & 0 & 0 \end{bmatrix}$

2.3 Rotor flux observer design of induction motor

The full order observer uses the induction motor model in stationary (α-β) reference frame, where the state variables are stator currents, $i_{\alpha s}$ and $i_{\beta s}$ and the rotor fluxes, $\Psi_{\alpha r}$ and $\Psi_{\beta r}$. The Figure 2.1 shows the block diagram of the speed adaptive flux observer using the above machine model, where the symbol "∧" means the estimated value.

Input voltage signal $v_{\alpha s}$ and $v_{\beta s}$ are measured from the machine terminal. If the speed signal ω_r in parameter matrix A is known, the flux and current can be solved from the state equations. However, if speed signal is not correct, there will be a deviation between the estimated state and the actual states. In the figure, the error is obtained from the comparison of the estimated currents with the actual machine terminal currents, the errors inject the auxiliary corrective signal eG through gain matrix G, as shown, so that matrix e tends to vanish. The full order state observer can be written as

$$\left(\frac{d}{dt}\right)\hat{x} = \hat{A}\hat{x} + BVs + GCe$$

$$\left(\frac{d}{dt}\right)\hat{x} = \hat{A}\hat{x} + BVs + GC(\hat{x} - x)$$

$$\left(\frac{d}{dt}\right)\begin{bmatrix} \hat{\imath}_s \\ \hat{\Psi}_r \end{bmatrix} = \begin{bmatrix} A_{11} & A_{12} \\ A_{21} & A_{22} \end{bmatrix}\begin{bmatrix} \hat{\imath}_s \\ \hat{\Psi}_r \end{bmatrix} + BV_s + GC\left(\begin{bmatrix} \hat{\imath}_s \\ \hat{\Psi}_r \end{bmatrix} - \begin{bmatrix} i_s \\ \Psi_r \end{bmatrix}\right) \tag{2.24}$$

Where, $i_s = [i_{\alpha s} \quad i_{\beta s}]^T$,

$\Psi_r = [\Psi_{\alpha r} \quad \Psi_{\beta r}]^T$,

$v_s = [v_{\alpha s} \quad v_{\beta s}]^T$,

A_{11}, A_{12}, A_{21} and A_{22} are sub-matrix of system matrix, A, given as

$A_{11} = -a_1 I$,

$A_{12} = a_2 I - a_3 \omega_r J$,

$A_{21} = a_5 I$,

$A_{22} = -a_4 I + \omega_r J$,

$C = [I \quad 0]$,

$I = \begin{bmatrix} 1 & 0 \\ 0 & 1 \end{bmatrix}$,

$$J = \begin{bmatrix} 0 & -1 \\ 1 & 0 \end{bmatrix} \text{ and}$$

$$G = \begin{bmatrix} g_1 & g_2 & g_3 & g_4 \\ -g_2 & g_1 & -g_4 & g_3 \end{bmatrix}^T$$

Where, G is the feedback gain matrix. Let the Eigen value of observer system matrix is also located at $(-x \pm y)$. Therefore G is calculated by the following equations:

$$g_1 = \frac{(x-a_4)a_2+(y+\omega_e-p\omega_r)a_3 p\omega_r}{{a_2}^2+(a_3 p\omega_r)^2} \quad (2.25)$$

$$g_2 = \frac{(x-a_4)a_3 p\omega_r-(y+\omega_e-p\omega_r)a_2}{{a_2}^2+(a_3 p\omega_r)^2} \quad (2.26)$$

and $g_3 = g_4 = 0$.

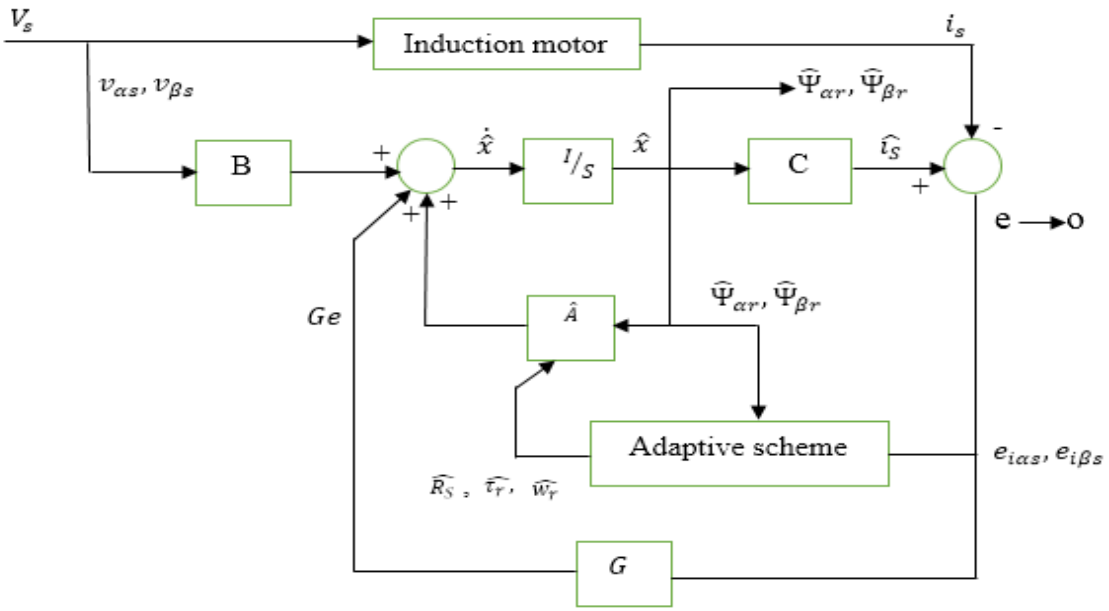

Fig. 2.1 Block diagram of adaptive rotor flux observer.

2.4 Conclusion

In this chapter, modelling of induction motor in the stationary reference frame has been described, where stator currents and rotor flux components are considered as a state variable. Design of rotor flux observer is also presented. Rotor flux observer is an estimator which estimates the stator currents and rotor flux using the terminal currents and voltages. Speed is then estimated by using the estimated stator currents and rotor flux.

Chapter 3

ADAPTIVE SCHEMES FOR SPEED ESTIMATION AND PARAMETER IDENTIFICATION FOR FIELD ORIENTED INDUCTION MOTOR DRIVE

3.1 Introduction

In order to eliminate the speed sensor from the drive, a speed estimation algorithm is used to estimate the speed. Several speed estimation algorithms and sensorless vector control schemes have been developed to avoid the use of speed sensor from the drive. Because a speed sensor increases cost and size of the drive and decreases reliability of the drive. A simple and low sensitivity speed sensorless direct rotor field oriented control (SDRFOC) scheme has been described. In this drive a hysteresis current control inverter has been used. The hysteresis band current controller has been extremely well known due to its straightforward usage, quick transient response, direct restricting of device peck current and functional inhumanity of dc connection voltage swell that allows a lower channel capacitor.

3.2 Adaptive schemes

3.2.1 Adaptive scheme for speed estimation

In order to eliminate rotational transducer from the viewpoint of expense, size of the drive, reliability and noise immunity. Therefore, it is essential to study and develop speed sensorless drive system. Several sensorless control schemes and speed estimation algorithms have been developed during the last few years. Motor speed is estimated by the following adaptive scheme [1, 13]. This scheme is also derived from Lyapunov's stability theorem:

$$W_r = (K_p + K_i/s)(e_{i\alpha s}\widehat{\Psi}_{\beta r} - e_{i\beta s}\widehat{\Psi}_{\alpha r}) \quad (3.1)$$

Where,

$e_{i\alpha s} = i_{\alpha s} - \hat{\imath}_{\alpha s}$,

$e_{i\beta s} = i_{\beta s} - \hat{\imath}_{\beta s}$,

K_p and K_i : Arbitrary positive constant.

$\hat{\Psi}_{\alpha r}$ and $\hat{\Psi}_{\beta r}$: Estimated rotor flux in stationary reference frame.

If $\hat{\Psi}_{\beta r}$ and $\hat{\Psi}_{\alpha r}$ are quadrature and direct axis components of the rotor flux in stationary reference frame as shown in Fig. 3.1, then the angle between resultant rotor flux and direct axis component of the rotor flux is calculated as:

$$\theta_{\Psi_r} = tan^{-1}\left(\frac{\hat{\Psi}_{\beta r}}{\hat{\Psi}_{\alpha r}}\right) \tag{3.2}$$

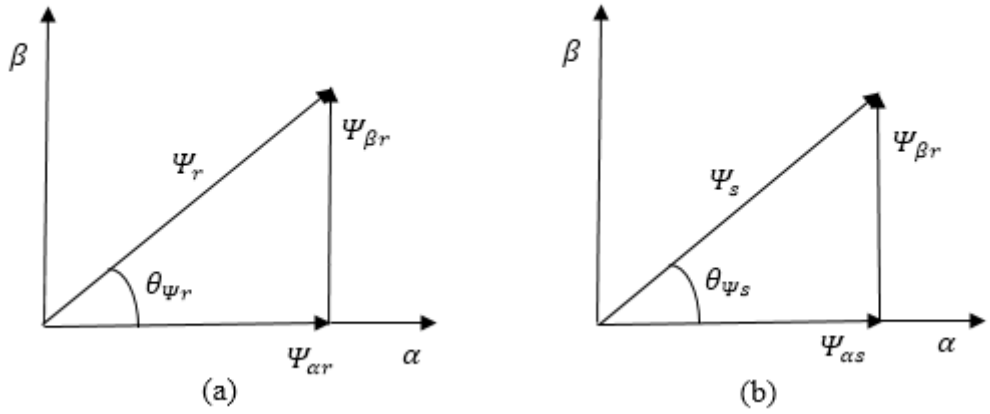

Fig. 3.1 Phasor diagram for rotor and stator flux components

If $\Psi_{\beta s}$ and $\Psi_{\alpha s}$ are quadrature and direct axis components of the stator flux in stationary reference frame as shown in fig. 3.1, then the electrical angle between resultant stator flux and direct axis component of the stator flux is calculated as:

$$\theta_{\Psi_s} = tan^{-1}\left(\frac{\Psi_{\beta s}}{\Psi_{\alpha s}}\right) \tag{3.3}$$

From the basic equations of induction motor in stationary reference frame the stator and rotor flux linkage are given by

$$\Psi_{\alpha s} = \int_0^t (v_{\alpha s} - R_s i_{\alpha s})\, dt \tag{3.4}$$

$$\Psi_{\beta s} = \int_0^t (v_{\beta s} - R_s i_{\beta s})\, dt \tag{3.5}$$

$$\Psi_{\alpha r} = \frac{L_r}{L_m}(\Psi_{\alpha s} - L_s \sigma i_{\alpha s}) \tag{3.6}$$

$$\Psi_{\beta r} = \frac{L_r}{L_m}(\Psi_{\beta s} - L_s \sigma i_{\beta s}) \tag{3.7}$$

The equations (3.4) and (3.4) show that the stator flux relies on the stator resistance and measured stator voltages and currents. The equations (3.6) and (3.7) show that the rotor flux relies on stator flux and the stator leakage inductance (L_s).

The line voltages, v_{ab}, v_{ac} and v_{bc} are also measured by using voltage sensors. The line currents, i_a, i_b and i_c are also measured by using current sensors. The measured line voltages are transformed into two phase stationary (α- β) reference frame, using Fig. 3.2, through the following equations. It is convenient to set $\theta = 0^0$.

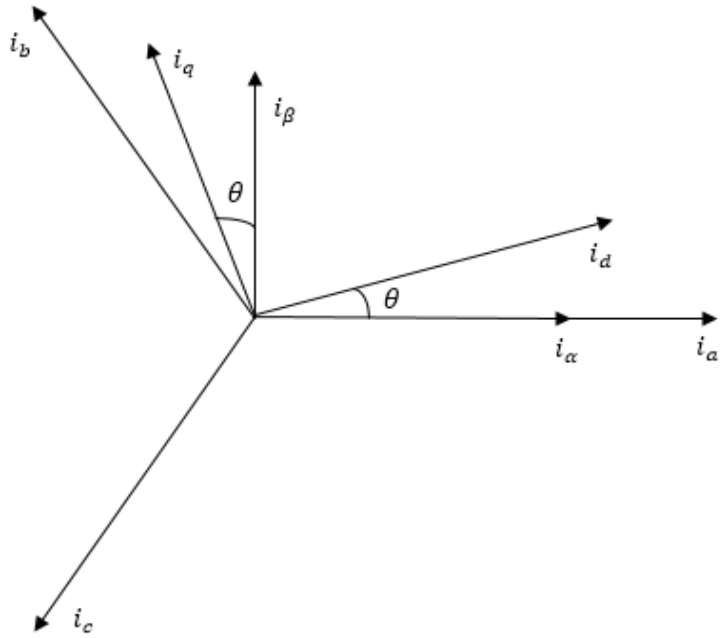

Fig. 3.2 Axis in the reference frames

$$v_{\alpha s} = \frac{2}{3}\left(v_a - \frac{1}{2}v_b - \frac{1}{2}v_c\right) = \frac{1}{3}(v_{ab} + v_{ac}) \tag{3.8}$$

$$v_{\beta s} = \left(\frac{2}{3}\right).\left(\frac{\sqrt{3}}{2}\right).(v_b - v_c) = \frac{1}{\sqrt{3}}v_{bc} \tag{3.9}$$

Similarly measured line currents are transformed into two phase stationary reference frame using the following equations.

$$i_{\alpha s} = \frac{2}{3}\left(i_a - \frac{1}{2}i_b - \frac{1}{2}i_c\right) = i_a \tag{3.10}$$

$$i_{\beta s} = \left(\frac{2}{3}\right).\left(\frac{\sqrt{3}}{2}\right).(i_b - i_c) = \left(\frac{1}{\sqrt{3}}i_a + \frac{2}{\sqrt{3}}i_b\right) \tag{3.12}$$

3.2.2 Adaptive scheme for stator and rotor resistance

There are also several methods to estimate the stator resistance and rotor time constant simultaneously [1]. The stator resistance and rotor time constant which vary with temperature. Hence it causes loss in the motor and decreases the motor efficiency and causes instability problem. To reduce these effect simultaneous estimation of stator resistance and rotor time constant is required. Stator resistance can be estimated by the given equation:

$$\left(\frac{d}{dt}\right)\hat{R}_s = -\lambda_1(e_{i\alpha s}\hat{\imath}_{\alpha s} + e_{i\beta s}\hat{\imath}_{\beta s}) \tag{3.13}$$

$$\left(\frac{d}{dt}\right)(1/\hat{\tau}_r) = \left(\frac{\lambda_2}{L_r}\right)\{e_{i\alpha s}(\hat{\Psi}_{\alpha r} - M\hat{\imath}_{\alpha s}) + e_{i\beta s}(\hat{\Psi}_{\beta r} - M\hat{\imath}_{\beta s})\} \tag{3.14}$$

Where,

$e_{i\alpha s} = i_{\alpha s} - \hat{\imath}_{\alpha s}$, $e_{i\beta s} = i_{\beta s} - \hat{\imath}_{\beta s}$, λ_1 and λ_2: arbitrary positive gain.

3.3 Sensorless direct rotor field oriented control scheme

A speed sensorless direct field oriented control (SDRFOC) scheme of three phase induction motor is depicted [5] in Fig. 3.3. The stator terminals current are measured and is converted into two phase stationary reference frame components using abc to α-β transformation. The rotor flux observer is an estimator which estimates rotor flux and stator current in stationary reference frame measuring terminal voltages and currents. The unit vectors are then derived from the stationary rotor flux signals.

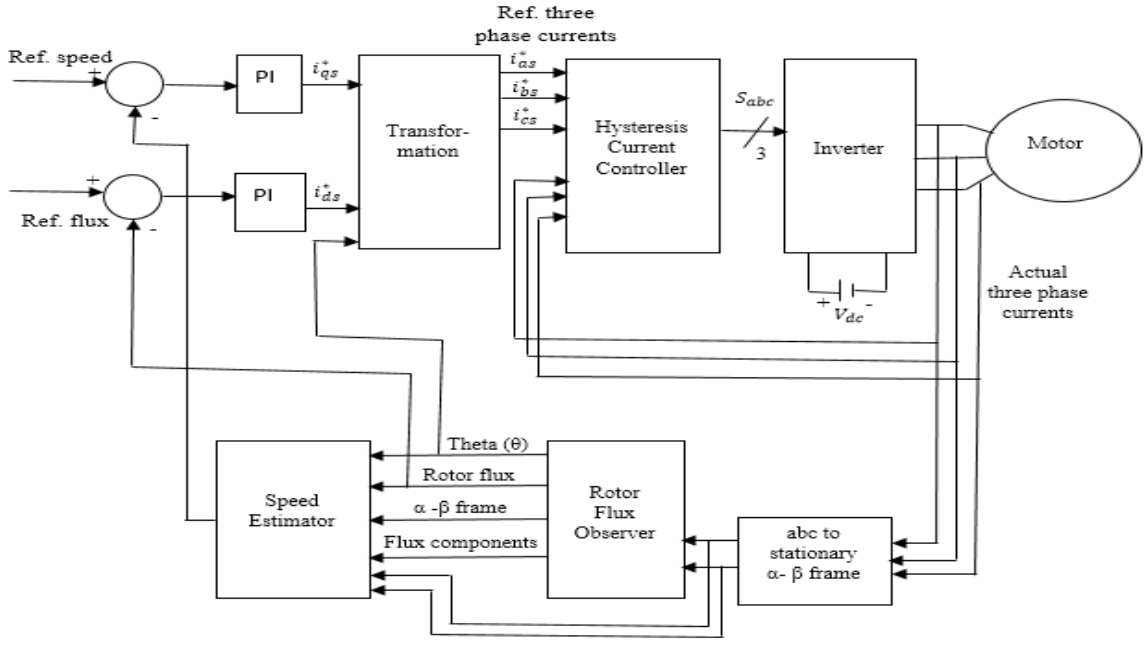

Fig. 3.3 Block diagram of sensorless direct rotor field oriented control scheme.

The speed control loop produces the torque component of stator current. The reference speed is contrasted with the estimated speed and the velocity error is fed to a PI controller in the speed control loop. The controller generates i_{qs}^{*} taking into account this speed error. Where, i_{qs}^{*} is known as torque component of stator reference current. So also a flux control loop is likewise included to improve the flux control accuracy. The flux component and torque component of stator current are converted to three phase quantities utilizing the unit vectors. These three phase currents are fed as reference values to the hysteresis band current controller. The switching signals for the inverter switches are generated from the controller, from the comparison of the current error signal with a fixed width hysteresis band.

3.4 Hysteresis band current control PWM

In industrial application, the current controlled PWM inverters are extensively used in ac motor drives. The main purpose of the control systems in current controlled inverters is to force the current vector in the three phase load according to a reference trajectory. This is presented in Fig. 3.4 for a half bridge inverter [13]. Where the reference current is contrasted with the actual phase current. When the actual current tries to go beyond the upper tolerance band, the upper switch in the half bridge is turned off and lower switch is turned on. Accordingly the output voltage changes from +0.5V_d to -0.5V_d and the current starts to decay. Similarly when the actual phase current tries to go beyond the lower tolerance band, the lower switch is turned off and the upper switch is turned on. As a result, output voltage transition from -0.5V_d to +0.5V_d and current starts to increase.

The conditions for switching the devices are:

Upper switch on: $(i^{*} - i) > HB$

Lower switch on: $(i^{*} - i) < -HB$

Where,

$i^{*} =$ Reference current;

$i =$ Actual phase current;

$HB =$ Hysteresis band.

For three phase inverter, a similar control scheme is used in all phases.

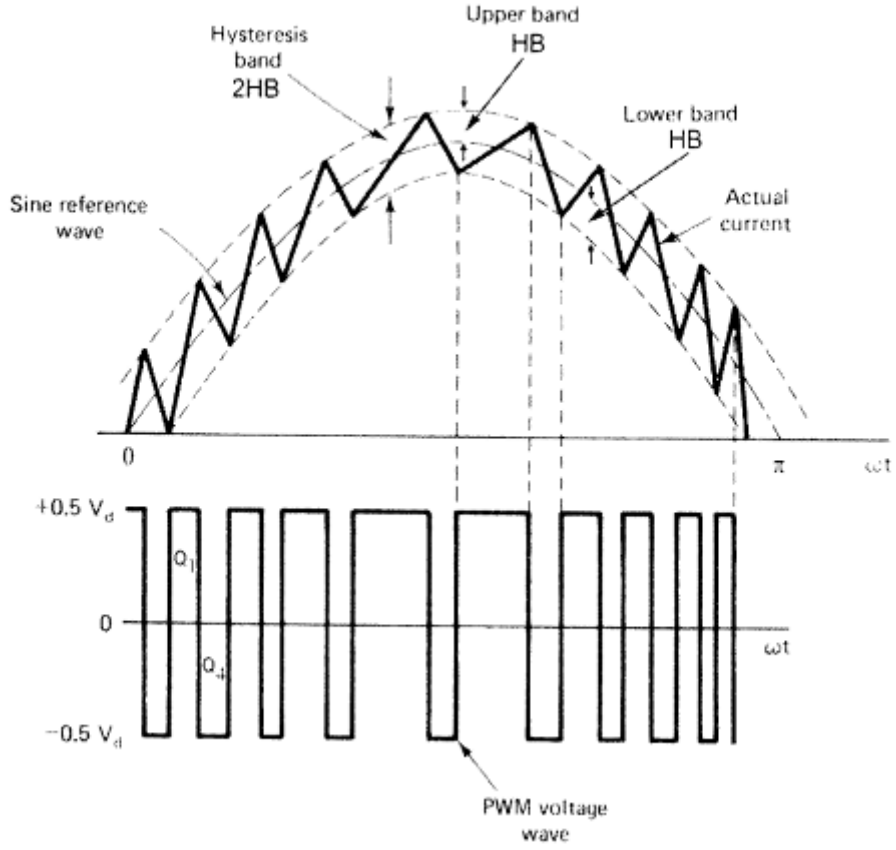

Fig. 3.4 Principle of hysteresis band current controller

3.5 Conclusion

In this chapter, the speed and motor parameters estimation schemes have been described and the basic principle of sensorless direct rotor field oriented control (SDRFOC) and hysteresis band current controlled have also been discussed. Speed of the motor is estimated by using estimation algorithm. In SDRFOC scheme a hysteresis band current controller is used because of its straightforward usage, quick transient response, direct restricting of device peck current and functional inhumanity of dc connection voltage swell that allows a lower channel capacitor.

Chapter- 4

AXES TRANSFORMATION

4.1 Introduction

Mathematical transformations are devices which make complex framework easy to study and easy to focus. In electrical machines analysis, a three phase variables to two phase variables transformation is applied to produce less complex expressions that provide more understanding into the cooperation of the distinctive parameters. In this chapter, the various transformations studied in the past have been presented.

4.2 General change of variables in transformations

Consider a symmetrical three phase induction machine with stationary three axes at 2π/3 angle apart as shown in Fig. 4.1. The real three phase supply system cane be represented by these three axes. Whereas, the two axes are representing two fictitious phases perpendicular to one other. The change of three phase variables to two phase variables [13] can be possible in such a way that the two phase variables are either in a stationary reference frame or in synchronously rotating reference frame. Transformation into a syncronously pivoted rotating reference frame is more common and it can be possible with the transformation of the three phase variables into two phase variables and after that transform these to synchronously moving reference frame. Speed of the stationary reference frame is zero, whereas speed of synchronously rotating reference frame is same as supply frequency. The stationary reference frame variables are appeared as a dc value in synchronously rotating reference frame instead of time varying quantities.

4.2.1 Transformation into a stationary reference frame

It is considered that the three phase axes and the two phase axes are in a stationary reference frame. Our aim is to transform the three phase (abc) variables to two phase (αβ0) variables. The relationship between three phase variables and two phase variables in stationary reference frame is given below and the transformation from three phase statiory reference frame to two phase stationary reference frame [13] can be understood from Fig. 4.1.

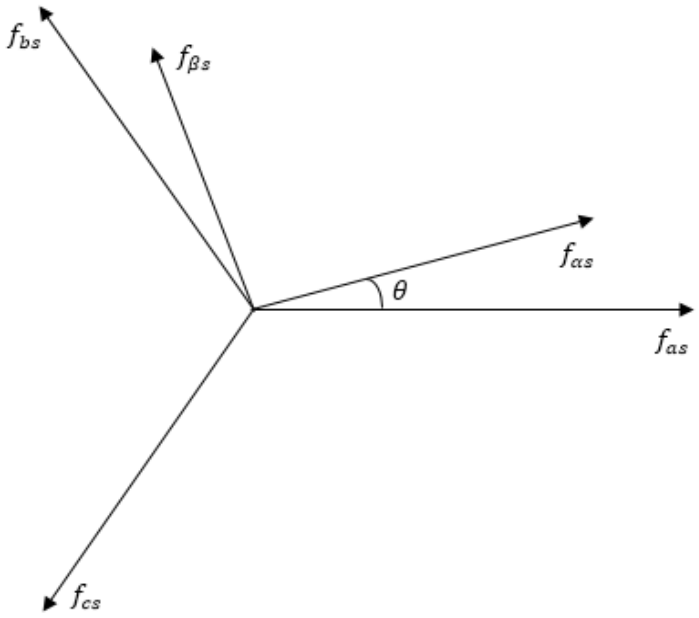

Fig. 4.1 Three-axes and two-axes in stationary reference frame

In the above diagram, Fig. 4.1, the voltage, current, or flux linkage can be denoted by f. The subscript s represents the variable associated with stationary reference frame. The angle, θ is the displacement of the two phase α-β winding, from the three phase, a-b-c winding. $f_{\alpha s}$ and $f_{\beta s}$ variables are perpendicular to each other. f_{as}, f_{bs} and f_{cs} may be considered as three phase variables in the stationary reference frame each displaced by $\frac{2\pi}{3}$ electrical degrees.

Transformation of the three phase variables in stationary reference frame to an arbitrary reference frame can be expressed in matrix form as:

$$\begin{bmatrix} f_{\alpha s} \\ f_{\beta s} \\ f_{0s} \end{bmatrix} = \frac{2}{3}\begin{bmatrix} \cos\theta & \cos\left(\theta - \frac{2\pi}{3}\right) & \cos\left(\theta + \frac{2\pi}{3}\right) \\ \sin\theta & \sin\left(\theta - \frac{2\pi}{3}\right) & \sin\left(\theta + \frac{2\pi}{3}\right) \\ \frac{1}{2} & \frac{1}{2} & \frac{1}{2} \end{bmatrix}\begin{bmatrix} f_{as} \\ f_{ab} \\ f_{ac} \end{bmatrix} \tag{4.1}$$

The corresponding inverse of Equation (4.1), is

$$\begin{bmatrix} f_{as} \\ f_{ab} \\ f_{ac} \end{bmatrix} = \begin{bmatrix} \cos\theta & \sin\theta & 1 \\ \cos\left(\theta - \frac{2\pi}{3}\right) & \sin\left(\theta - \frac{2\pi}{3}\right) & 1 \\ \cos\left(\theta + \frac{2\pi}{3}\right) & \sin\left(\theta + \frac{2\pi}{3}\right) & 1 \end{bmatrix}\begin{bmatrix} f_{\alpha s} \\ f_{\beta s} \\ f_{0s} \end{bmatrix} \tag{4.2}$$

It is convenient to set $\theta = 0$, so that the α-axis is aligned with the a-axis. Therefore the Equation (4.1) will be written as

$$\begin{bmatrix} f_{\alpha s} \\ f_{\beta s} \\ f_{0s} \end{bmatrix} = \frac{2}{3}\begin{bmatrix} 1 & -\frac{1}{2} & -\frac{1}{2} \\ 0 & -\frac{\sqrt{3}}{2} & \frac{\sqrt{3}}{2} \\ \frac{1}{2} & \frac{1}{2} & \frac{1}{2} \end{bmatrix}\begin{bmatrix} f_{as} \\ f_{ab} \\ f_{ac} \end{bmatrix} \tag{4.3}$$

and Equation (4.2) will be simplified to

$$\begin{bmatrix} f_{as} \\ f_{ab} \\ f_{ac} \end{bmatrix} = \begin{bmatrix} 1 & 0 & 1 \\ -\frac{1}{2} & -\frac{\sqrt{3}}{2} & 1 \\ -\frac{1}{2} & \frac{\sqrt{3}}{2} & 1 \end{bmatrix}\begin{bmatrix} f_{\alpha s} \\ f_{\beta s} \\ f_{0s} \end{bmatrix} \tag{4.4}$$

Equations (4.3) and (4.4) shows that the magnitude of the phase quantities, voltages and currents, in the three phase stationary reference frame (a-b-c) variables and two phase stationary reference frame (d-q) variables remain the same. In this transformation, it is considred that the number of turns in each phase of the three phase winding and the two phase winding are same.

4.2.2 Transformation into rotating reference frame

The rotating frame of reference can have any speed of rotation subjected to the requirment of the system. If the speed of the roatating reference frame matches wih the frequencey of excitation current, then all the transformed variables of instataneous values will appear as constant quantity. Thus it can be stated that if an observer moves along with the same speed then the space vector looks as three dimension with steady state. The speed of rotation for the reference frame must be same as the observer. For two dimensional variables any two independent basic space vectors can be taken as reference. These are denoted by another pair of orthogonal d-q axes. The zero-sequence elements remains unchanged. The stationary reference frame a-b-c variables converted to the rotating reference frame d-q variables occurs in two steps, i.e., first transforming to stationary α-β variables and then to rotating d-q variables. The axes transformation from abc to dq0 is shown in Fig. 4.2.

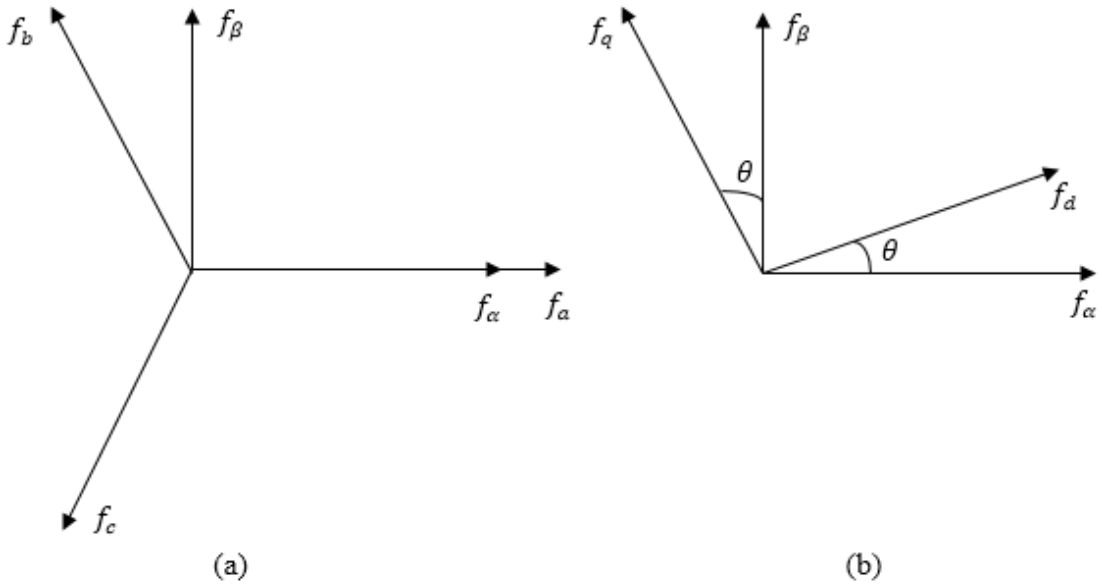

Fig. 4.2 Shows steps of the a-b-c to rotating d-q axes transformation: (a) a-b-c to stationary α- β axes and (b) stationary α-β to rotating d-q axes.

The equation for the stationary reference frame α-β variables to rotating reference frame d-q variables transformation [13] is given in Equation (4.5). Utilizing geometry, the relation between the stationary α-β axes and rotating d-q axes can be expressed as:

$$\begin{bmatrix} f_d \\ f_q \end{bmatrix} = \begin{bmatrix} \cos\theta & \sin\theta \\ -\sin\theta & \cos\theta \end{bmatrix} \begin{bmatrix} f_\alpha \\ f_\beta \end{bmatrix} \tag{4.5}$$

The angle, θ, is the displacement between the two phase stationary reference frame α-β and two phase rotating reference frame d-q. The angular speed, ω (t), of the rotating reference frame d-q can be represented with theta (θ) function. The initial values are written as

$$\theta(t) = \int_0^t \omega(t)\, dt + \theta(0) \tag{4.6}$$

Three phase voltages and currents in stationary reference frame can be obtained by applying two phase stationary reference frame, α-β to three phase stationary reference frame, a-b-c transformation equations as above explained

$$\begin{bmatrix} f_a \\ f_b \\ f_c \end{bmatrix} = \begin{bmatrix} 1 & 0 \\ -\frac{1}{2} & -\frac{\sqrt{3}}{2} \\ -\frac{1}{2} & \frac{\sqrt{3}}{2} \end{bmatrix} \begin{bmatrix} f_\alpha \\ f_\beta \end{bmatrix} \tag{4.7}$$

The three phase voltage or current quantities in stationary reference frame are represented by f_a, f_b and f_c and the two-phase voltage or current quantities in stationary reference frame are represented by f_α and f_β.

4.3 Conclusion

Transformation from abc to dq0 is discussed in this chapter. It is desired for any balanced 3-ϕ system. Complexity of calculations are reduced by three phase variables to two phase variable transformation. For a single instant of time only one arrangement of estimations can be taken to obtain voltage, current, power factor and active power. Also, from estimations taken at two continuous moments can give the frequency of the three phase AC power supply.

Chapter-5

SIMULATION RESULTS AND DISCUSSION

5.1 Introduction

A Simulink model of speed sensorless vector control for three phase induction motor has been developed in MATLAB, Simulink. Different speed, current and flux graph have been plotted in different speed and load torque.

5.2 Results and discussion

A 50 Hp, 440 V, 4-pole, 50Hz three phase induction motor is used for the simulation studies. The motor parameters are as shown in table1. The simulation results of the sensorless vector control drive employing HBPWM controller with an inverter and an IM with the following specifications are considered.

The dc link voltage V_{dc} should be around $1.453V_L$ where V_L denotes r.m.s value of line voltage. Sampling time (T_S): 2μs, Hysteresis Band width of HBPWM current controller is 0.5.

TABLE - 1

INDUCTION MOTOR PARAMETERS

Parameters	Value
Stator resistance	0.087 Ω
Rotor resistance	0.228 Ω
Stator inductance	35.5 mH
Rotor inductance	35.5 mH
Mutual inductance	34.7 mH
No. of poles	4
Moment of inertia	1.662 kg/m^2
Friction co-efficient	0.1 N/m/s

The simulation results for the drive system with two PI controllers are presented under the following conditions.

1. Constant reference speed without load (free acceleration).V_L

2. Constant reference speed with load.

5.2.1 Without load (free acceleration)

Fig. 5.1 shows the simulation response of actual motor speed, estimated motor speed and error between actual speed and estimated speed for a constant speed reference of 80 rad/sec. The reference flux is kept at 0.98 web and the load torque is kept at zero N-m. At starting motor accelerating and finally reached to steady state. It is also observed that after a small time the estimated speed always followed the reference speed, because the speed controller knows the estimated speed one only. The actual speed converged to the reference speed.

Fig. 5.2 shows the simulation response of the actual and estimated α-axis stator currents and the errors between them. At starting motor currents are uneven because of circuit inductance. Starting motor currents are four to five times the steady state current. At steady state the current value is 28A. Under steady state actual and estimated currents match with each other. Therefore, the error between them is zero under steady state operation of the motor, as shown in Fig. 5.2.

Fig. 5.3 shows the simulation response of actual and estimated β- axis stator currents and the current errors between these two. Similar to the α- axis stator current, the actual and estimated β-axis stator currents match with each other under steady state operation of the motor.

Fig. 5.4 shows the simulation response of actual and estimated α-axis rotor flux and the error between them. At starting rotor fluxes are increasing and then reaches to reference value. The estimated rotor flux and actual rotor flux settle to the reference value within 0.98 web. The reference speed is kept at 80 rad/sec and load torque is kept at zero N-m. Similarly, Fig. 5.6 shows the simulation response of actual and estimated q-axis rotor flux. Actual rotor flux and estimated rotor flux match with each other at steady state operation of the motor.

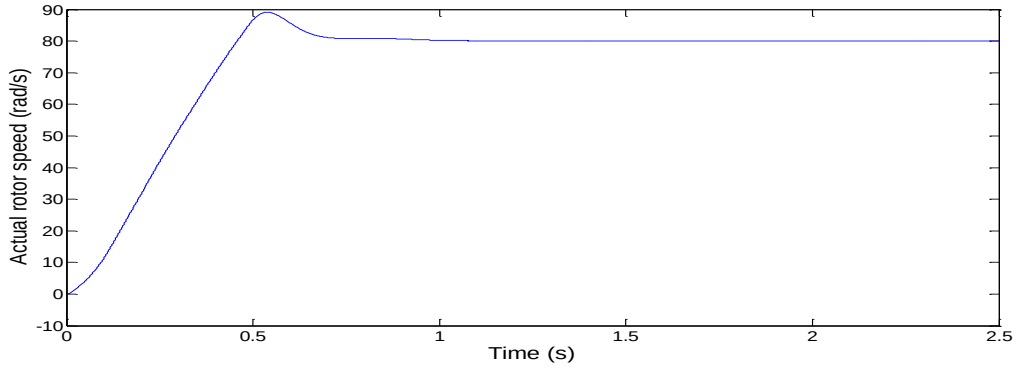

(a)

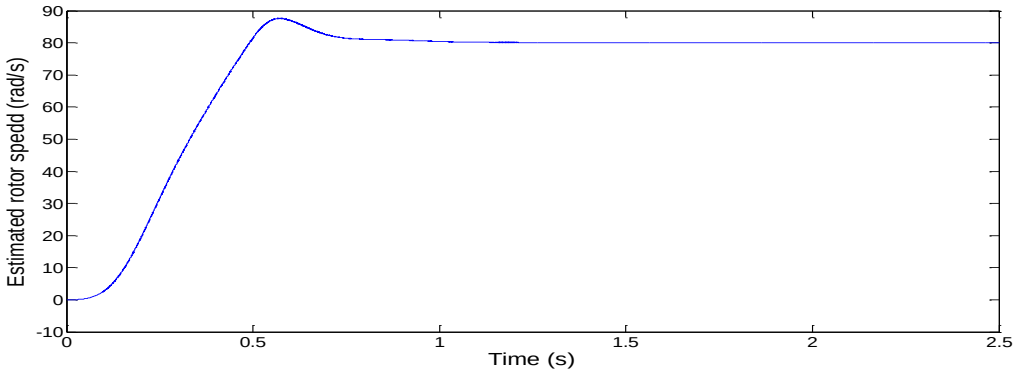

(b)

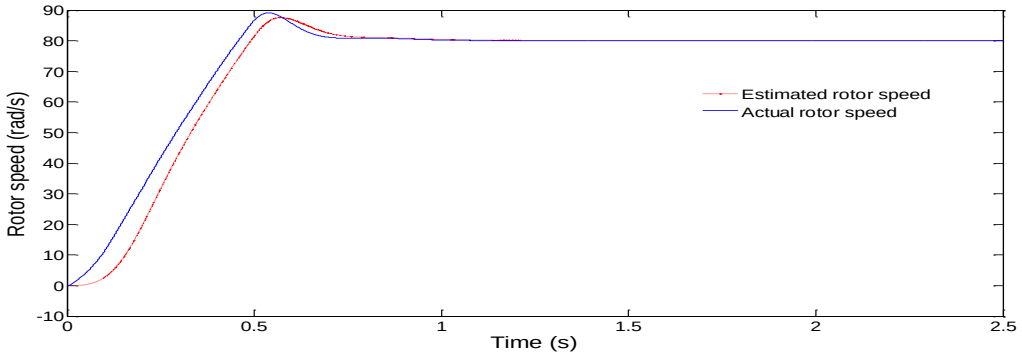

(c)

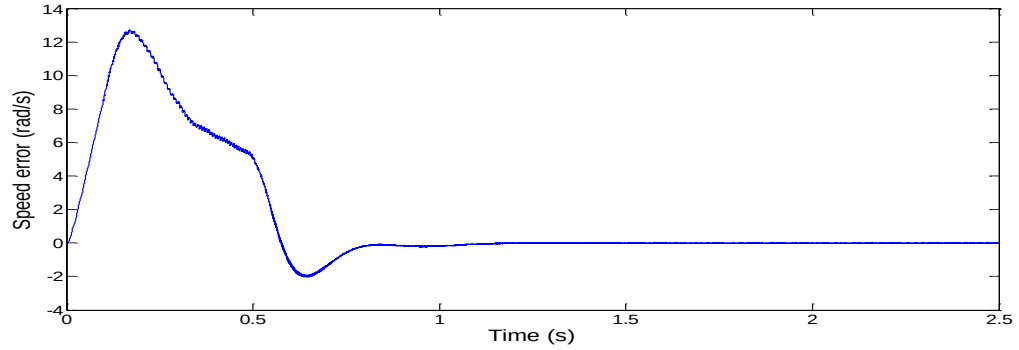

(d)

Fig. 5.1 Simulation response of rotor speed: (a) Actual rotor speed (ω_r), (b) Estimated rotor speed ($\hat{\omega}_r$), (c) Actual and estimated rotor speed (ω_r, $\hat{\omega}_r$) and (d) Speed error.

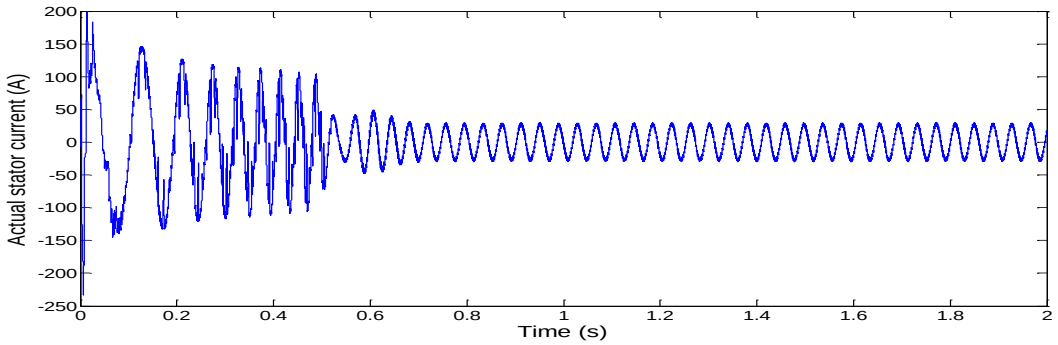

(a)

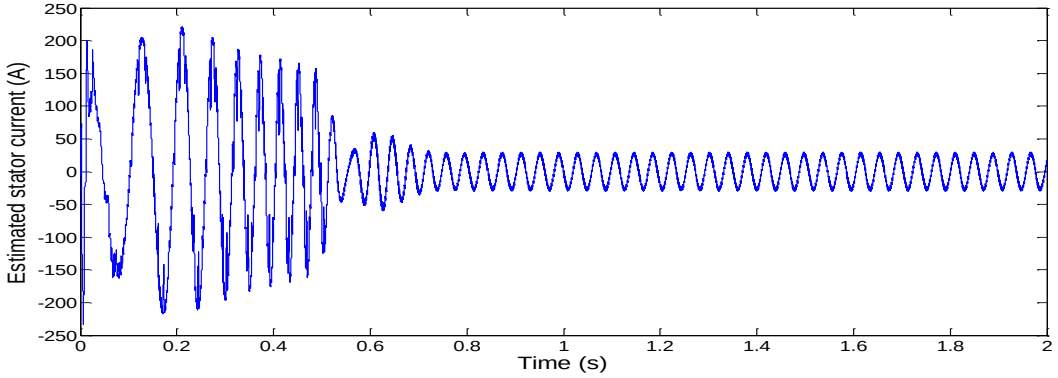

(b)

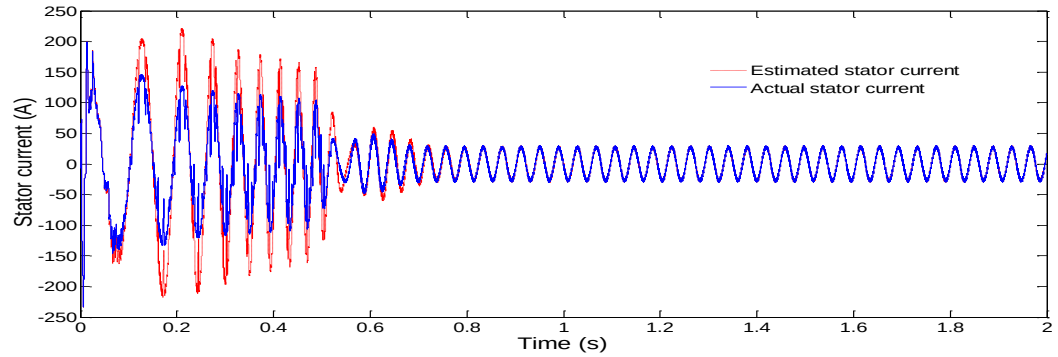

(c)

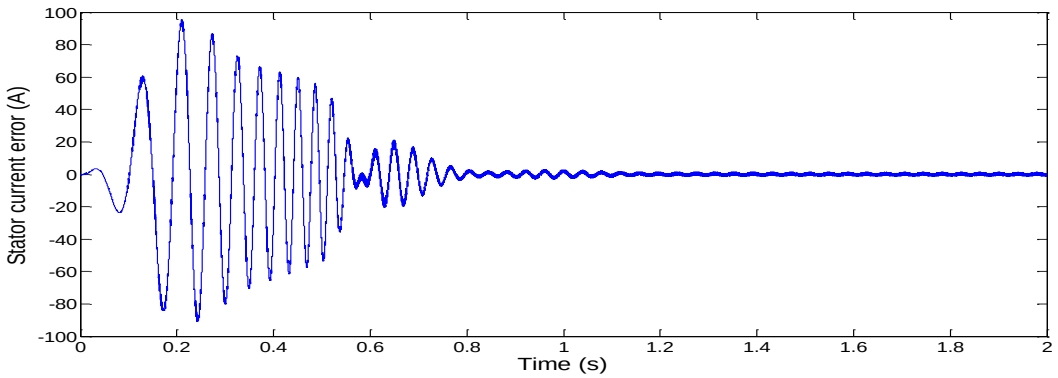

(d)

Fig. 5.2 Simulation response of α-axis stator current: (a) Actual stator current ($i_{\alpha s}$), (b) Estimated stator current ($\hat{\imath}_{\alpha s}$), (c) Both actual and estimated stator current ($i_{\alpha s}$, $\hat{\imath}_{\alpha s}$) and (d) α-axis stator current error.

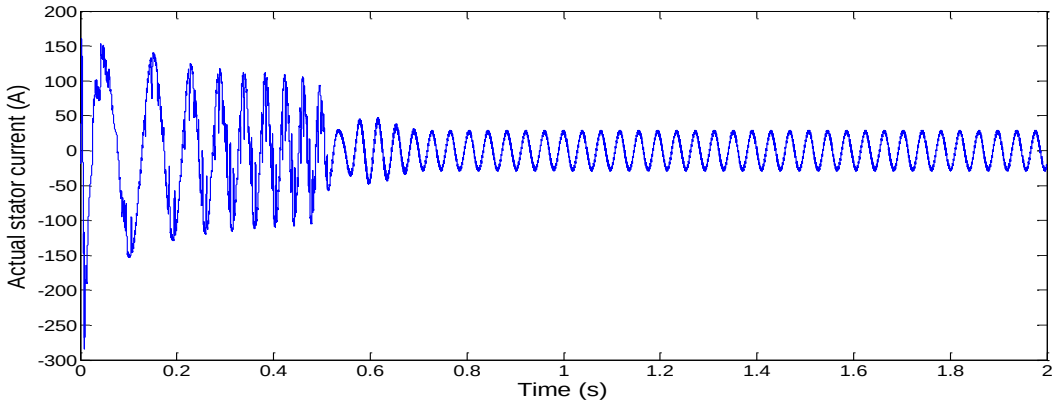

(a)

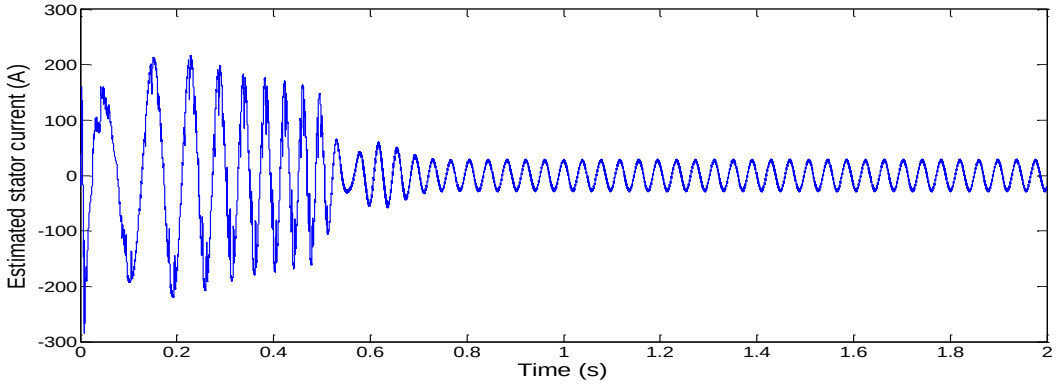

(b)

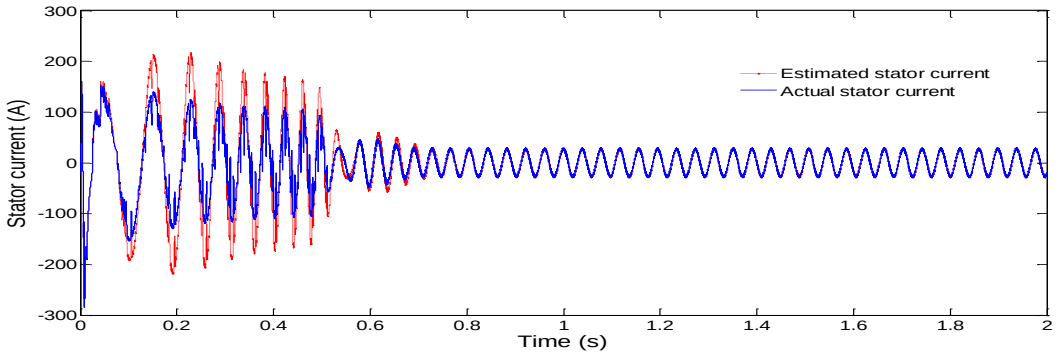

(c)

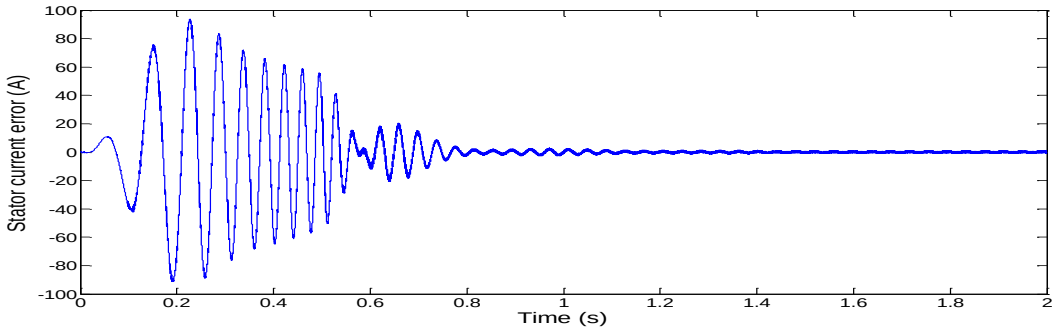

(d)

Fig. 5.3 Simulation response of β-axis stator current: (a) Actual stator current ($i_{\beta s}$), (b) Estimated stator current ($\hat{\imath}_{\beta s}$), (c) Both actual and estimated stator current ($i_{\beta s}$, $\hat{\imath}_{\beta s}$) and (d) β-axis stator current error.

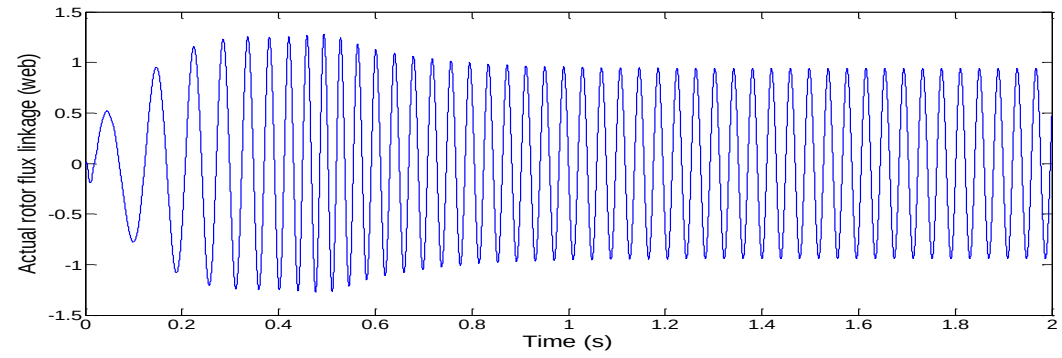

(a)

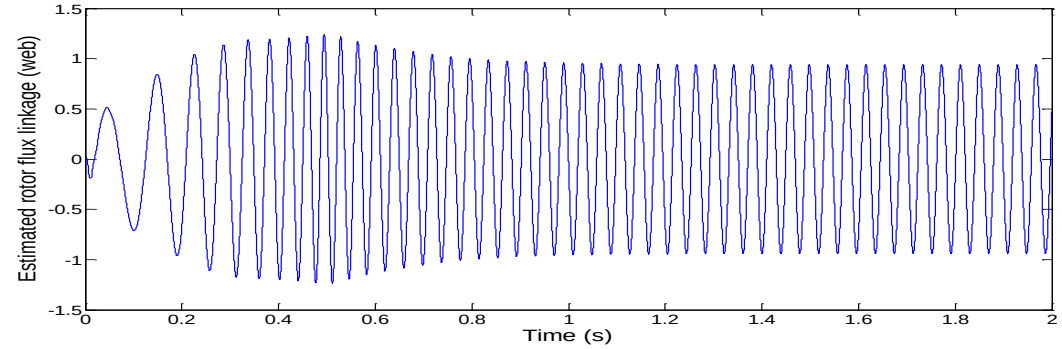

(b)

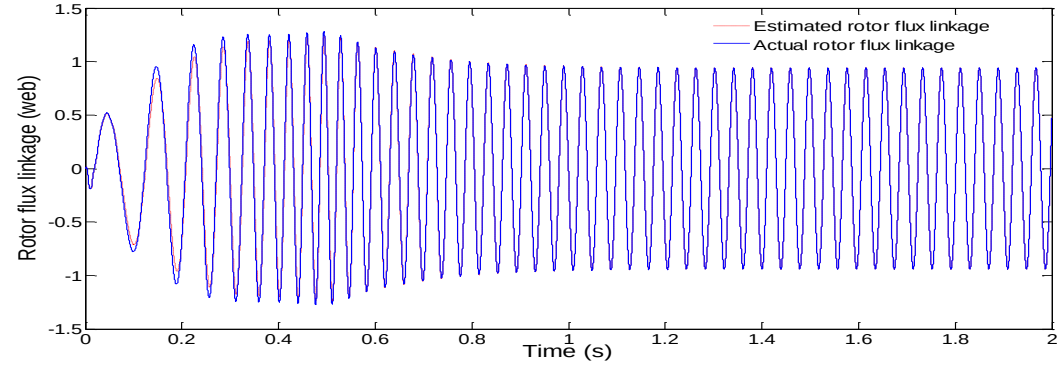

(c)

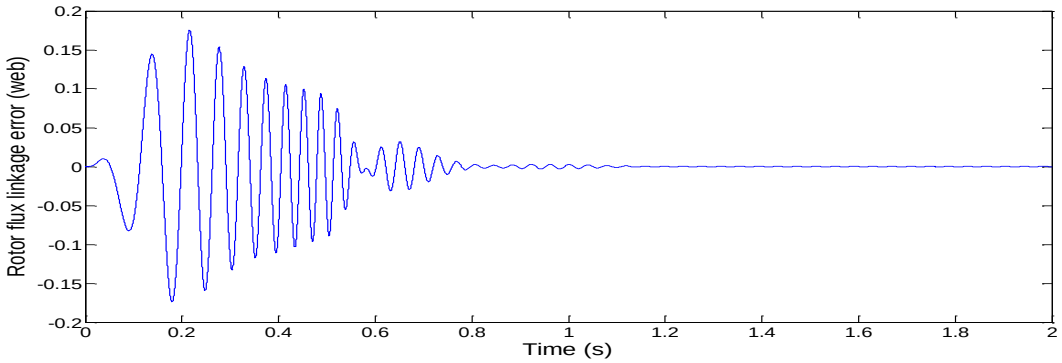

(d)

Fig. 5.4 Simulation response of α-axis rotor flux linkage: (a) Actual rotor flux linkage ($\Psi_{\alpha r}$), (b) Estimated rotor flux linkage ($\widehat{\Psi}_{\alpha r}$), (c) Both actual and estimated rotor flux linkage ($\Psi_{\alpha r}$, $\widehat{\Psi}_{\alpha r}$) and (d) α-axis rotor flux linkage error.

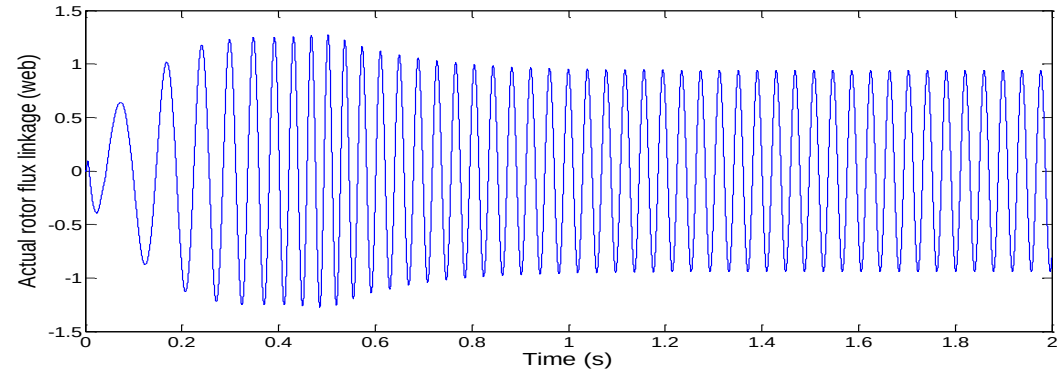

(a)

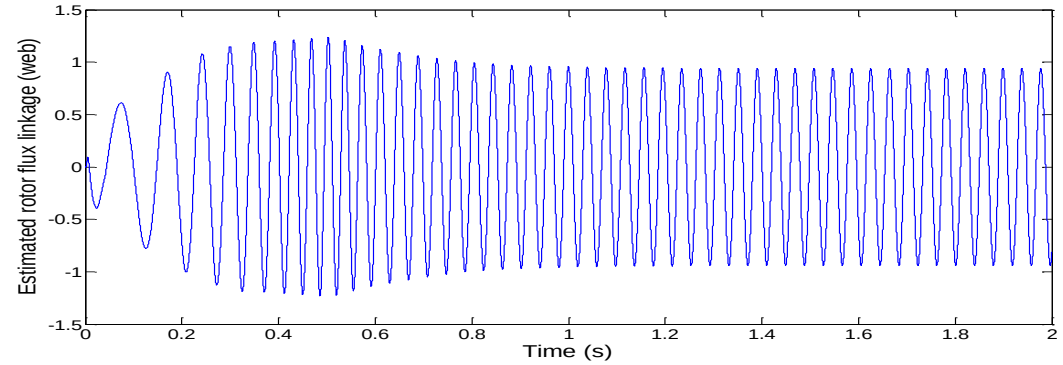

(b)

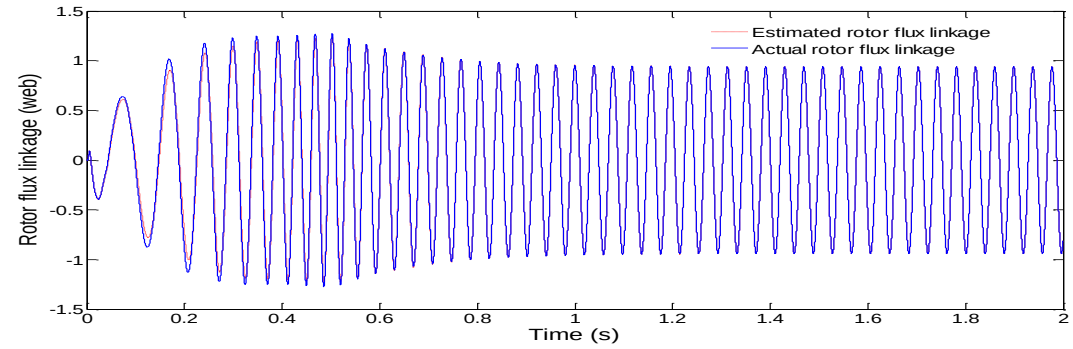

(c)

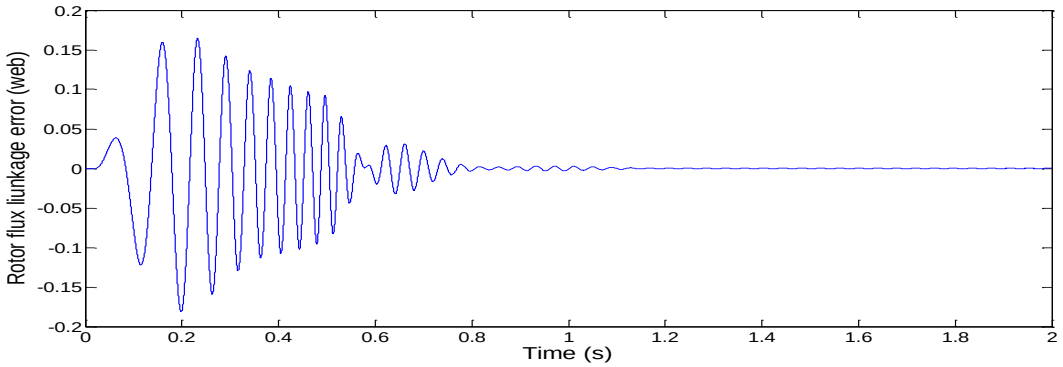

(d)

Fig. 5.5 Simulation response of β-axis rotor flux linkage: (a) Actual rotor flux linkage ($\Psi_{\beta r}$), (b) Estimated rotor flux linkage ($\widehat{\Psi}_{\beta r}$), (c) Both actual and estimated rotor flux linkage ($\Psi_{\beta r}, \widehat{\Psi}_{\beta r}$) and (d) β-axis rotor flux linkage error.

5.2.2 Under load

Fig. 5.6 shows the simulation response of actual motor speed, estimated motor speed and error between actual speed and estimated speed for a constant speed reference of 100 rad/sec. The reference flux is kept at 0.98 web and the load torque is kept at 25 N-m. At starting motor is accelerating and finally reaches to steady state. It is also observed that after a small time the estimated speed always followed the reference speed, because the speed controller knows the estimated speed one only. The actual speed converged to the reference speed.

Fig. 5.7 shows the simulation response of the actual and estimated α-axis stator currents and the errors between them. At starting the motor currents are uneven because of circuit inductance. Under steady state actual and estimated currents match with each other. Therefore, the error between them is zero under steady state operation of the motor, as shown in Fig. 5.7.

Fig. 5.8 shows the simulation response of actual and estimated β-axis stator currents and the current errors between these two. Similar to the α- axis stator current, the actual and estimated β-axis stator currents match with each other under steady state operation of the motor.

Fig. 5.9 shows the simulation response of actual and estimated α-axis rotor flux and the error between them. The estimated rotor flux and actual rotor flux settle to the reference value within 0.98 web. The reference speed is kept at 100 rad/sec and load torque is kept at 25 N-m. Similarly, Fig. 5.10 shows the simulation response of actual and estimated β-axis rotor flux. The rotor flux starts increasing at starting and reaches to the reference value after a small delay.

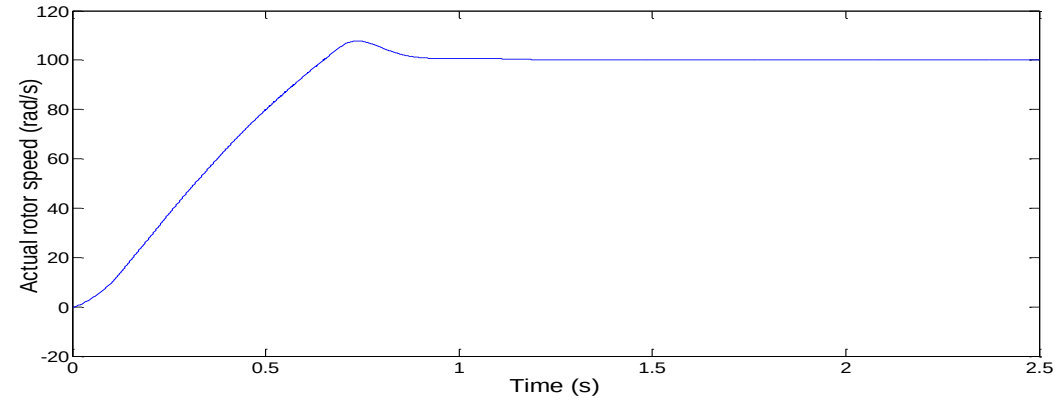

(a)

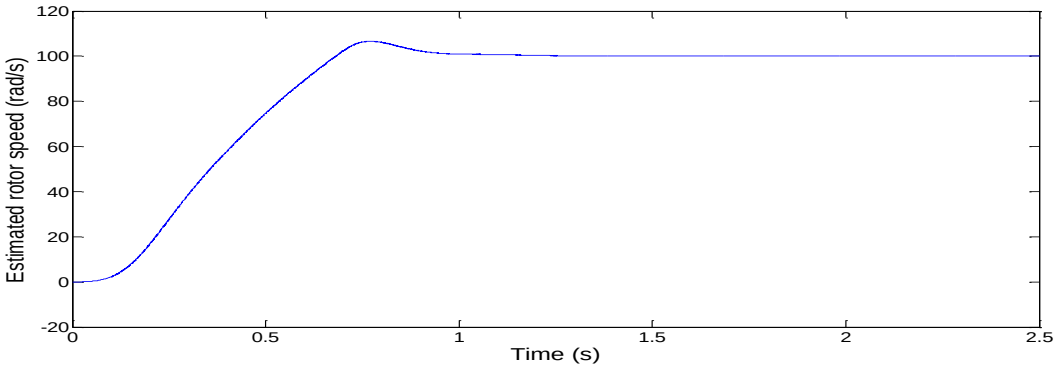

(b)

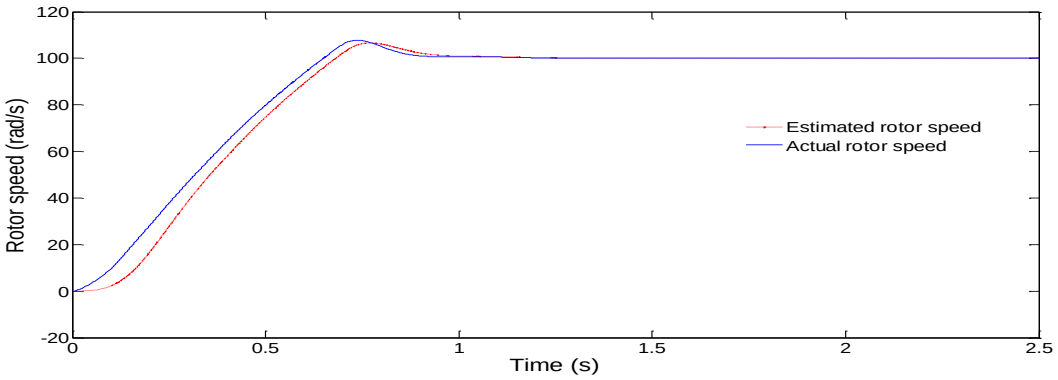

(c)

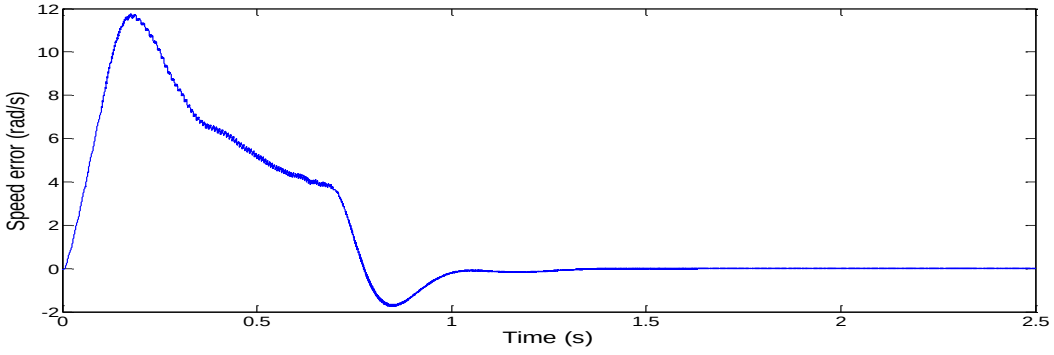

(d)

Fig. 5.6 Simulation response of rotor speed: (a) Actual rotor speed (ω_r), (b) Estimated rotor speed ($\hat{\omega}_r$), (c) Actual and estimated rotor speed (ω_r , $\hat{\omega}_r$) and (d) Speed error.

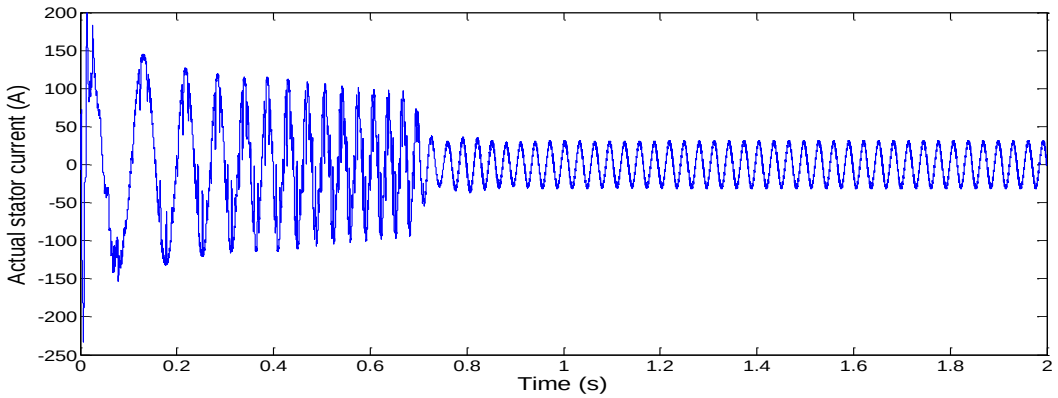

(a)

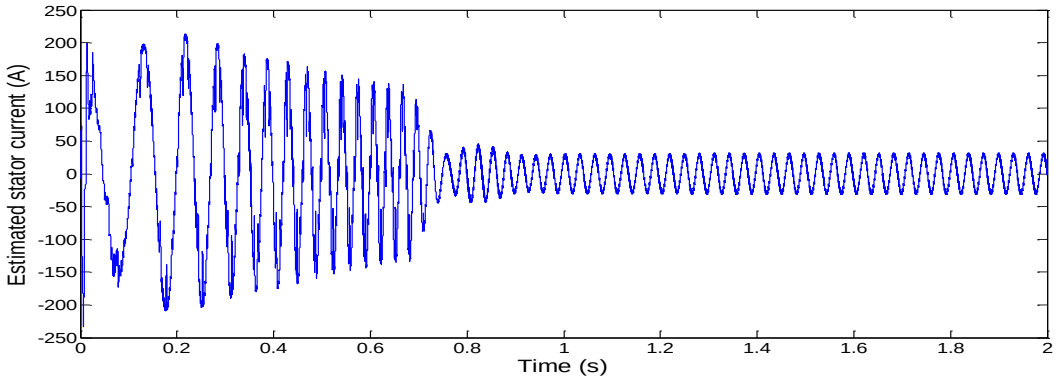

(b)

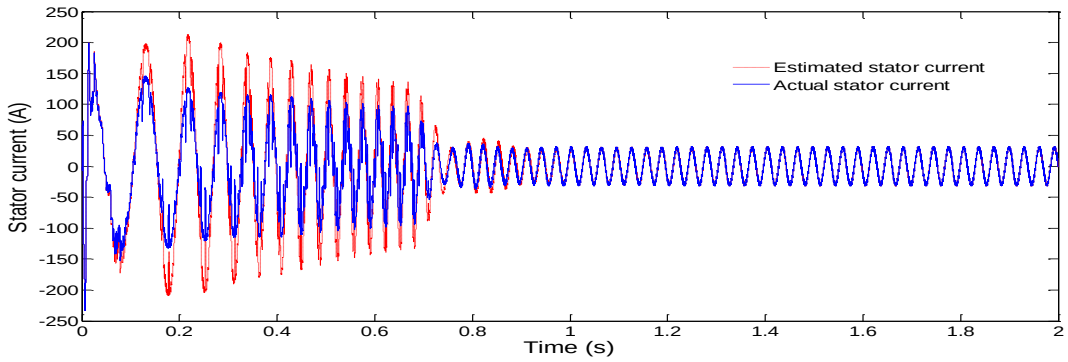

(c)

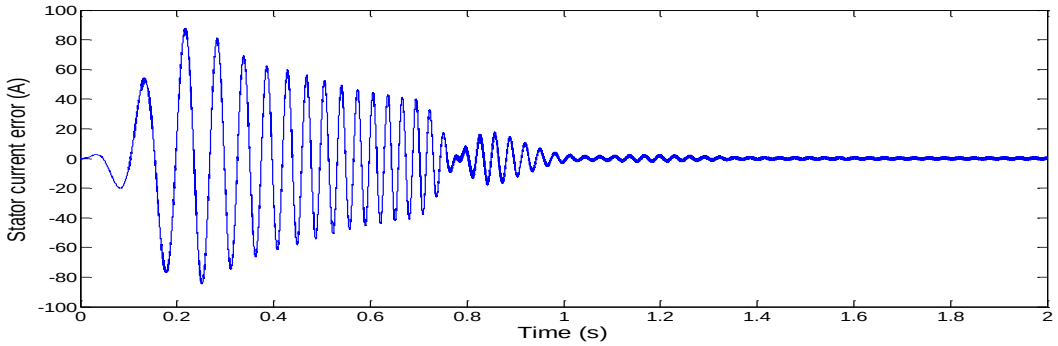

(d)

Fig. 5.7 Simulation response of α-axis stator current: (a) Actual stator current ($i_{\alpha s}$), (b) Estimated stator current ($\hat{\imath}_{\alpha s}$), (c) Both actual and estimated stator current ($i_{\alpha s}$, $\hat{\imath}_{\alpha s}$) and (d) α-axis stator current error.

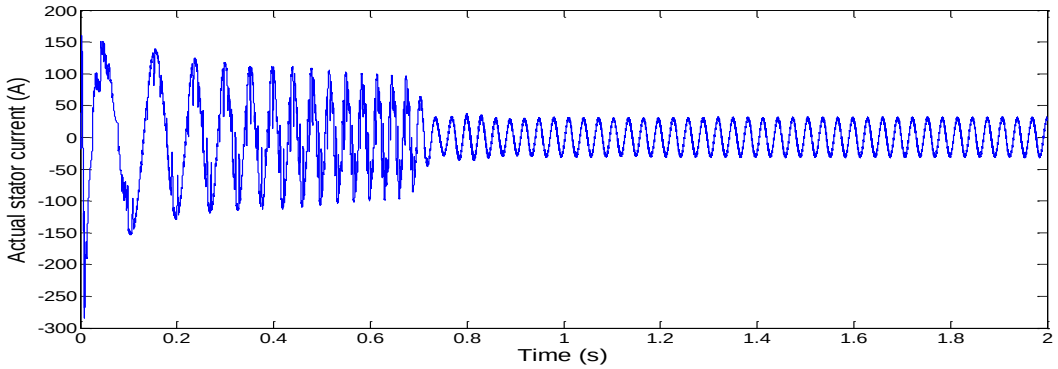

(a)

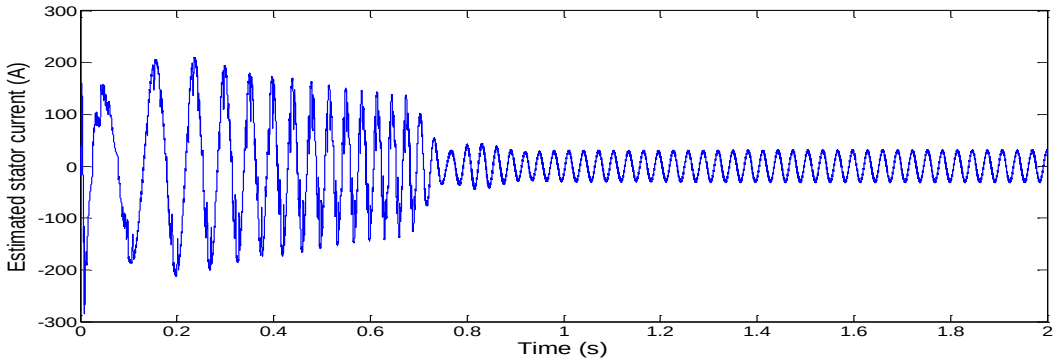

(b)

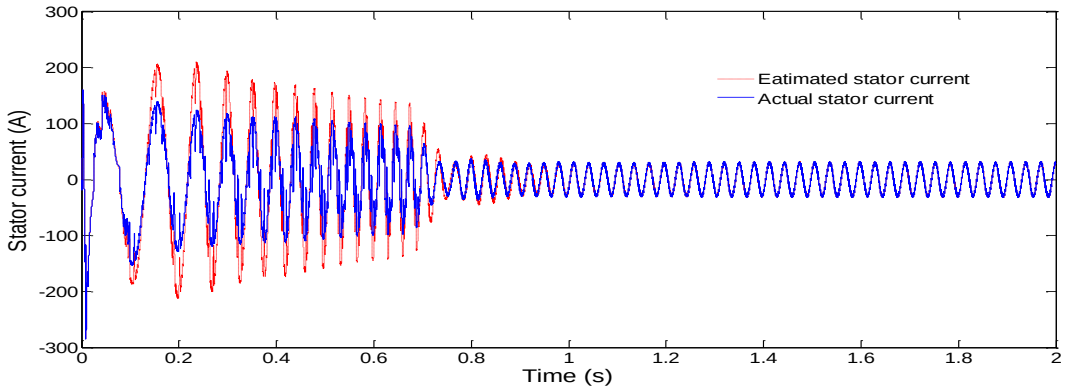

(c)

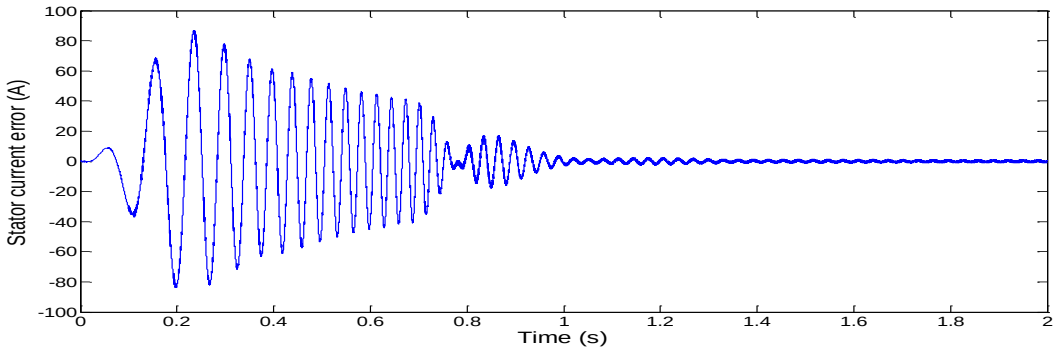

(d)

Fig. 5.8 Simulation response of β-axis stator current: (a) Actual stator current ($i_{\beta s}$), (b) Estimated stator current ($\hat{\imath}_{\beta s}$), (c) Both actual and estimated stator current ($i_{\beta s}$, $\hat{\imath}_{\beta s}$) and (d) β-axis stator current error.

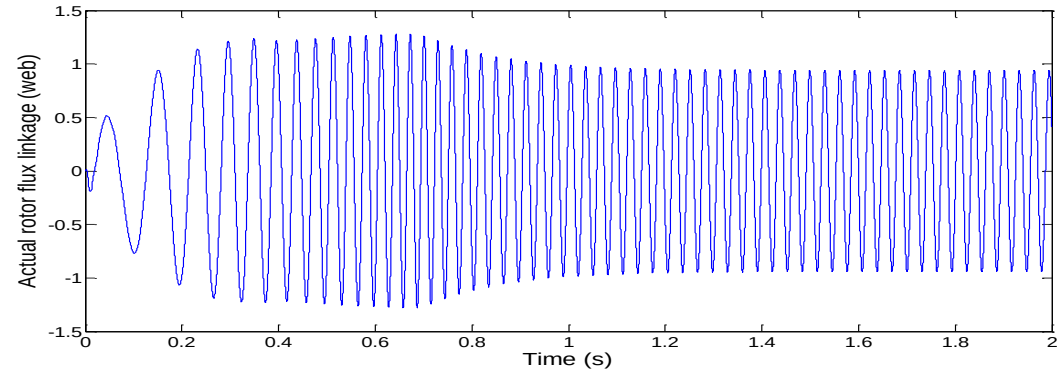

(a)

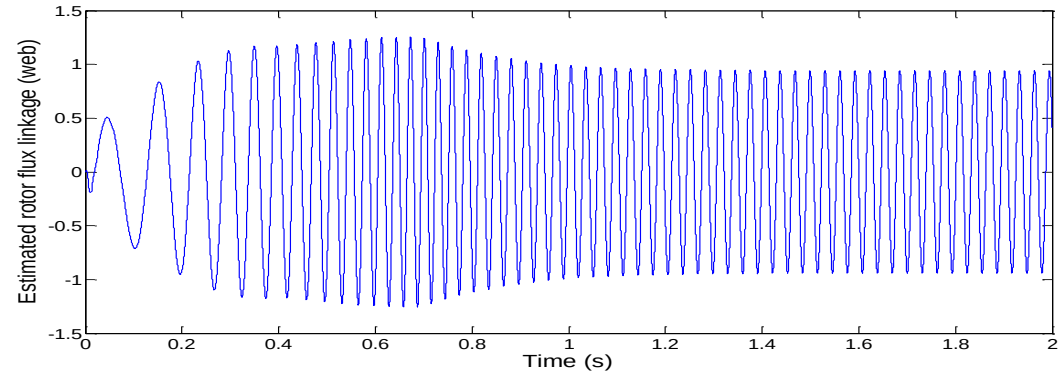

(b)

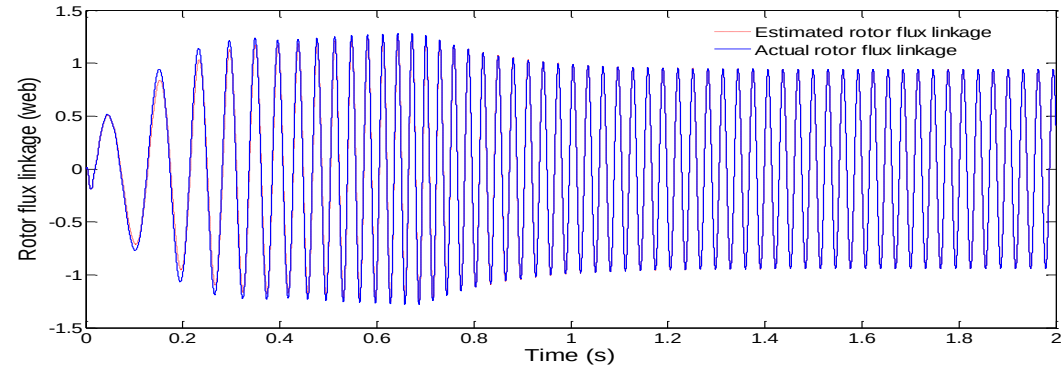

(c)

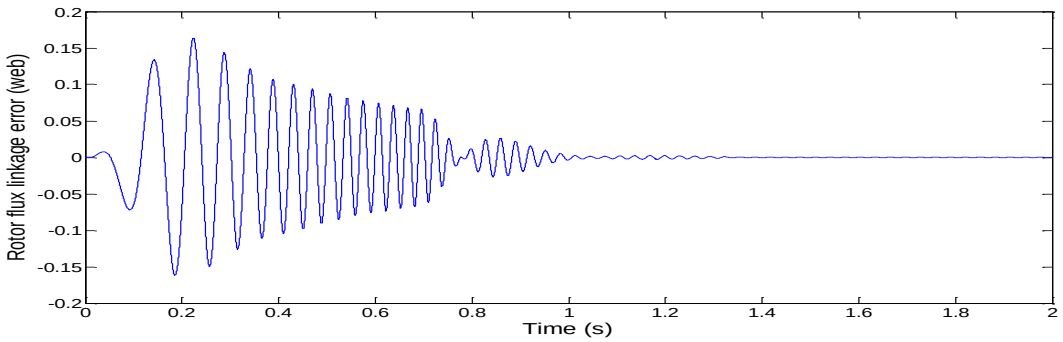

(d)

Fig. 5.9 Simulation response of α-axis rotor flux linkage: (a) Actual rotor flux linkage ($\Psi_{\alpha r}$), (b) Estimated rotor flux linkage ($\widehat{\Psi}_{\alpha r}$), (c) Both actual and estimated rotor flux linkage ($\Psi_{\alpha r}$, $\widehat{\Psi}_{\alpha r}$) and (d) α-axis rotor flux linkage error.

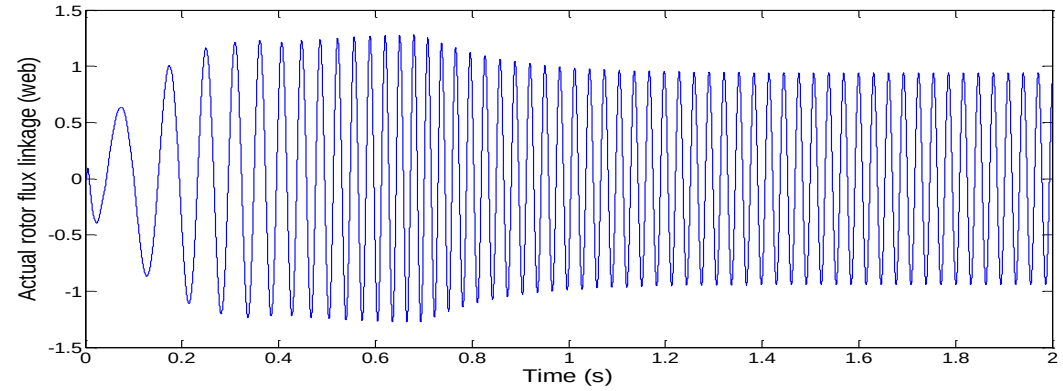

(a)

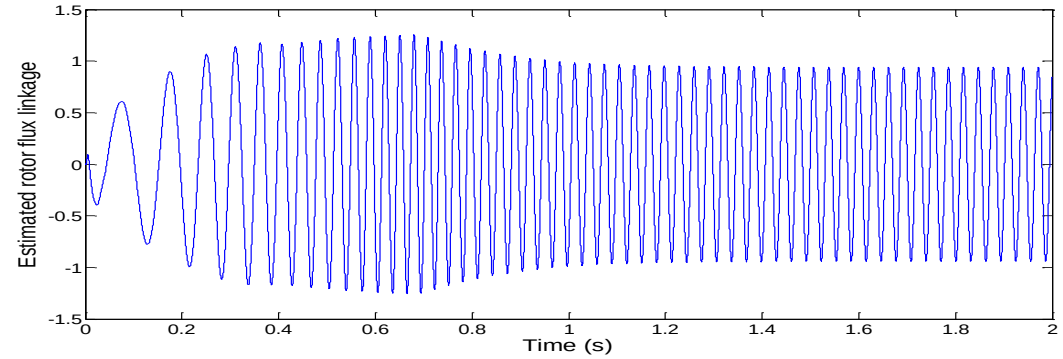

(b)

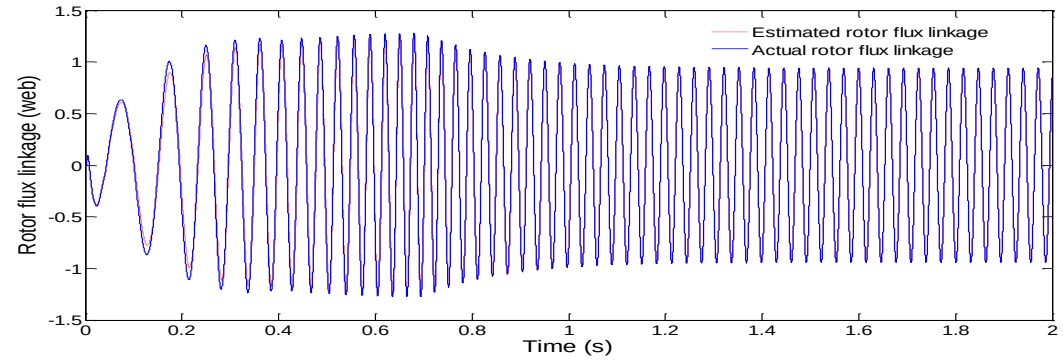

(c)

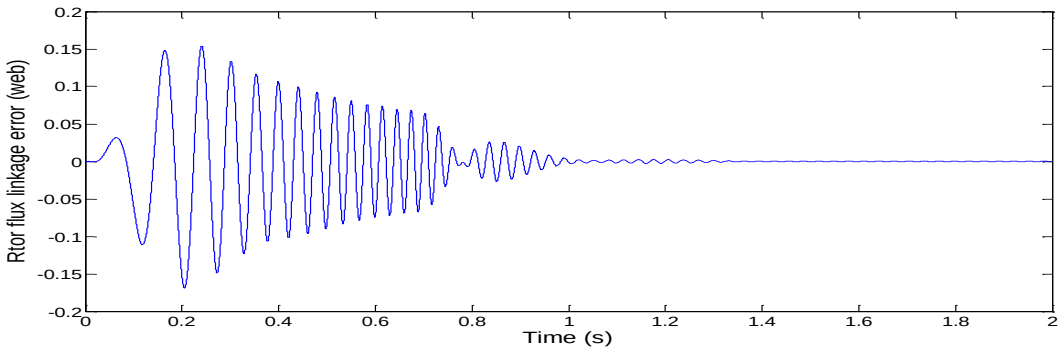

(d)

Fig. 5.10 Simulation response of β-axis rotor flux linkage: (a) Actual rotor flux linkage ($\Psi_{\beta r}$), (b) Estimated rotor flux linkage ($\widehat{\Psi}_{\beta r}$), (c) Both actual and estimated rotor flux linkage ($\Psi_{\beta r}$, $\widehat{\Psi}_{\beta r}$) and (d) β-axis rotor flux linkage error.

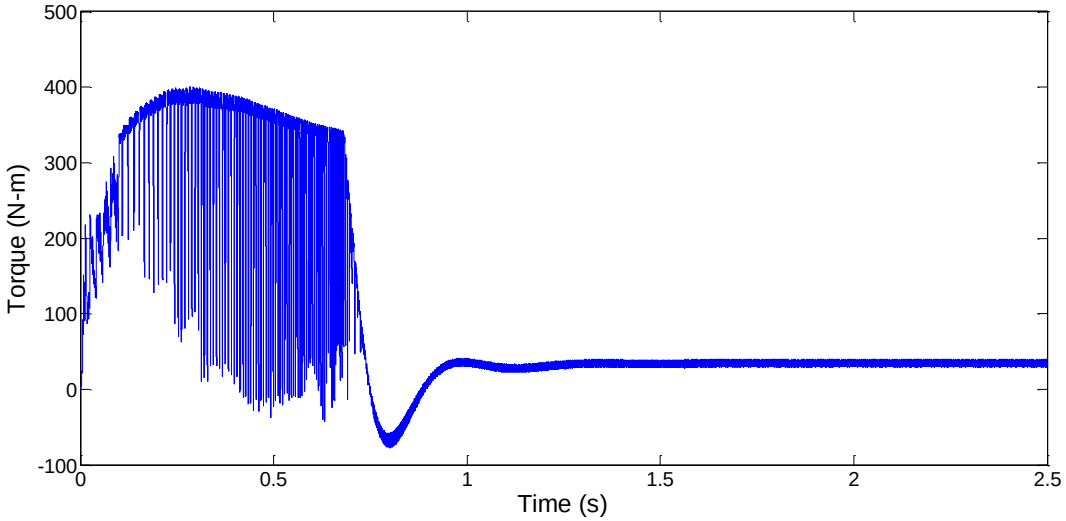

Fig. 5.11 Simulation response of developed torque (T_e)

5.3 Conclusion

In this chapter, simulation results of induction motor drive system based on speed sensorless vector control have been presented. All the simulation results have been observed with two PI controller, one is used in speed control loop and another one is used in speed estimation algorithm. At starting the stator currents are more in comparison to that of in steady state, because it is necessary to develop high torque for increasing the motor speed. Error between the estimated and actual values of a variable in steady state is zero.

Chapter-6

GENERAL CONCLUSION

6.1 Conclusion

The objective of this project was to develop a speed sensorless drive for three phase induction motor based on a rotor flux observer. The convergence of rotor flux to reference value is made faster by the proper selection of observer gain matrix and the speed estimation accuracy can be improved by the observer. The speed tracking objective is achieved succesfully and the system can operate stably in the whole operating range. The validity of the speed tracking objective has been verified by the simulation results.

6.2 Scope for future work

The direction of future work may be divided in the following aspect:

1. The motor parameters variation was not considered through the research works. Therefore, study the motor parameters variation in different speed, still remains remarkable study.
2. The model of induction motor adopted here does not consider magnetic saturation. Therefore investigation of proposed speed sensorless system in field weakening, still remains valid in this condition.
3. It would be interesting to study the performance of sensorless vector control and to compare it with conventional vector control.
4. The present work can be extended to estimate the rotor flux using Extended kalman filter. A comparative study can be made with both type of flux estimators to examine their suitability for induction motor.

REFERENCES

[1] H. Kubota and K. Matsuse, "Speed sensorless field-oriented control of induction motor with rotor resistance adaptation," IEEE Trans. Ind. App., vol. 30, no. 5, pp. 1219-1224, October 1994.

[2] R. Bojoi, P. Guglielmi and G. M. Pellegrino, "Sensorless direct field-oriented control of three-phase induction motor drives for low-cost applications," IEEE Trans. Ind. Appl., vol. 44, no. 2, pp. 475-481, Mar. 2008.

[3] C. Schauder, "Adaptive speed identification for vector control of induction motor without rotational transducers," IEEE Trans. Ind. App., vol. 28, no. 5, pp. 1054-1061, October 1992.

[4] B. Renukrishna and S. Shanifa Beevi, "Sensorless vector control of induction motor drives using rotor flux observer," 2012 IEEE International Conference on Power Electronics, Drives and Energy Systems December 16-19, 2012, Bengaluru, India.

[5] W. Chen and D. G. Xu, "Stability analysis of speed adaptive flux observer for induction motor speed sensorless vector control," International Conference on Electrical Machines and Systems, 2010.ICEMS'10, pp. 689-693, October 2010, Incheon.

[6] G. C. Verghese and S. R. Sanders, "Observers for flux estimation in induction machines," IEEE Trans. Ind. Elec., vol. 35, no.1, pp. 85-94, Feb. 1998.

[7] X. Zou, P. Zhu, Y. Kang and J. Chen, "Speed Identification for speed sensorless vector control of induction motors based on voltage decoupling control principle," Electrical Machines and Drives Conference, 2003.IEMDC'03. IEEE International, vol.1, pp. 269 -273, June 2003.

[8] R. Krishnan and A.S. Bharadwaj, "A review of parameter sensitivity and adaptation in indirect vector controlled induction motor drive systems," Power Electronics Specialists Conference, 1990.PESC'90, PP. 560-566, 1990.

[9] S. Tamai and H. Sugimoto, "Secondary resistance identification of an induction motor applied model reference adaptive system and its characteristics," IEEE Trans. Ind. Appl., vol. 23, no. 5, pp. 296-303, march 1987.

[10] H. Kubota, I. Sato, Y. Tamura, K. Matsuse, H. Ohta, and Y. Hori, "Regenerating mode low speed operation of sensorless induction motor drive with adaptive

observer", IEEE Trans. Ind. App., vol. 38, no. 4, pp. 1081-1086, Jul./Aug. 2002.

[11] Y. R. Kim, S. K. Sul, and M. H. Park, "Speed sensorless vector control of induction motor using extended Kalman filter," IEEE Trans. Ind. Appl., vol. 30, no. 5, pp. 1225–1233, Sep./Oct. 1994.

[12] M. Montanari, S. M. Peresada, C. Rossi and A. Tilli, "speed sensorless control of induction motor based on reduced order Adaptive Observer," IEEE Trans. Ind. Appl., vol. 15, no. 6, pp. 1049- 1064, Nov. 2007.

[13] B. K. Bose, "Modern Power Electronics and AC Drives," Prentice- Hall, New Jersey, 2002.

[14] O. Barambones, A. J. Garrido and F. J. Maseda, "Integral sliding mode controller for induction motor based on field oriented control theory," IEEE Trans. Control Theory Appl., vol. 1, no. 3, pp. 786- 794, May 2007.

[15] A. Sabanovic and D. B. Izosimov, "Application of sliding modes to induction motor control," IEEE Trans. Ind. Appl., vol. IA-17, no. 1, pp. 41–49, Jan./Feb. 1981.

[16] F. J. Lin and C. M. Liaw, "Control of indirect field-oriented induction motor drives considering the effects of dead-time and parameter variations," IEEE Trans. Ind. Electronics, vol. 40, no. 5, pp. 486– 495, Oct. 1993.

[17] F. Z. Peng and T. Fukao, "Robust speed identification for speed sensorless vector control of induction motors," IEEE Trans. Ind. Appl., vol. 30, no. 5, pp. 1234–1240, Sep./Oct. 1994.

[18] M. Hinkkanen and J. Luomi, "Stabilization of generating mode operation in sensorless induction motor drives by full order flux observer design," IEEE Trans. Ind. Electronics, vol. 51, no. 6, pp. 1318–1328, Dec. 2004.

[19] M. Hinkkanen, "Analysis and design of full order flux observers for sensorless induction motor ," IEEE Trans. Ind. Appl., vol. 51, no. 5, pp. 1033- 1040, Oct. 2004.

[20] E. D. Mitronikas and A. N. Safacas, " An improved sensorless vector control method for an induction motor drive ," IEEE Trans. Ind. Electronics, vol. 52, no. 6, pp. 1660-1668, Dec. 2005.

APENDIX- A

Table- 2

Proportional cum Integral controller parameters

loop	K_p	K_i
Speed control loop	40	200
Rotor flux observer	0.05	45